Universidade de Aveiro
2013
Departamento de Engenharia de Materiais e Cerâmica

Filipe André Heliodoro Franco

Upscaling challenges for LDH-containing active protection coatings

Universidade de Aveiro
2013
Departamento de Engenharia de Materiais e Cerâmica

Filipe André Heliodoro Franco

Upscaling challenges for LDH-containing active protection coatings

Tese apresentada à Universidade de Aveiro para cumprimento dos requisitos necessários à obtenção do grau de Mestre em Engenharia de Materiais, realizada sob a orientação científica do Doutor Mikhail Zheludkevich, Investigador Principal do Departamento de Engenharia de Materiais e Cerâmica da Universidade de Aveiro

“Não to mandei eu? Esforça-te, e tem bom ânimo; não te atemorizes, nem te espantes; porque o Senhor teu Deus está contigo, por onde quer que andares”. Josué1:9 Bíblia Sagrada

o júri

Presidente

Professor Doutor Mário Guerreiro Silva Ferreira
Professor Catedrático, Universidade de Aveiro

Professor Doutor Dmitry Victorovitch Evtyugin
Professor Associado com agregação, Universidade de Aveiro

Doutor Mikhail Larionovich Zheludkevich
Equiparado a Investigador Principal, Universidade de Aveiro

Agradecimentos

Os meus agradecimentos vão para o meu orientador Dr. Mikhail Zheludkevich pela orientação e apoio dado em todo o momento na realização deste trabalho bem como para os orientadores Jose Ramirez Flores e Magali Wainer pela incondicional formação, orientação e integração no mundo industrial. Um agradecimento especial ao aluno de doutoramento Jorge Carneiro pela orientação, disponibilidade e paciência dada no laboratório.
Ao Dr. Andrei Salak, Dra. Susana Olhero e Dr. Alexandre Bastos pela disponibilidade de me formar em determinados tópicos desenvolvidos nesta tese bem como aos meus colegas de laboratório.
Aos meus colegas e amigos de curso principalmente o José Ribeiro e o Ricardo Laranjeira pelas partilhas, risadas, apoio condicional e irmandade que tiveram ao longo da realização desta tese. Para os meus amigos chegados agradeço os momentos que tiveram e aconselhamento dado, nomeadamente ao Paulo Silva, Jonatas Braz, Samuel Campos e John Pallister.
Por fim, o meu agradecimento vai para a família nomeadamente ao meu pai, mãe e irmão pelo tremendo amor e suporte dado durante em todo o momento e por fim ao meu Deus por amar imensuravelmente este seu filho.

palavras-chave

Hidróxidos duplos lamelares, corrosão, testes de corrosão acelerada, revestimento, difração de raios X, dispersão, proteção ativa

Resumo

O principal objetivo deste trabalho é estudar os desafios associados a um revestimento de proteção ativa contendo (HDL) hidróxidos duplos lamelares quando passado de uma escala laboratorial para industrial. Dois tipos de revestimento foram estudados contendo HDL com gluconato intercalado nas galerias com e sem adição de alginato à sua superfície. Foi estudada a dispersão de ambas as partículas numa formulação polimérica e foi demonstrado que o alginato permite uma dispersão mais rápida e efetiva bem como uma melhor compatibilidade na matriz. A possível aglomeração dos HDL na formulação foi avaliada através de análises do tamanho de partícula e demonstrou uma razoável compatibilidade entre o pigmento e o polímero. Os revestimentos foram estudados com testes normalizados de corrosão acelerada e com técnicas eletroquímicas, demonstrando a proteção ativa conferida pelos HDL. As propriedades protetoras do revestimento foram estudadas através de espetroscopia de impedância eletroquímica e revelou que a adição de HDL permite proteção ativa nos revestimentos, maiores valores de impedância e um atraso no aparecimento de novas constantes de tempo. O período de vida útil do pigmento HDL bem como dos HDL na formulação do revestimento foram estudados controlando a estrutura cristalina dos HDL através da técnica de difração de raios-X. Nenhumas alterações na estrutura dos HDL foram observados durante o armazenamento em ar, no entanto, no entanto, para a formulação, houve uma alteração no espaçamento basal o que pode estar associado à intercalação de espécies aniónicas da formulação nas galerias dos HDL.

Chegou-se à conclusão que a compatibilidade dos HDL com a formulação do revestimento pode ser melhorada com a modificação dos pigmentos com alginato considerando a aplicação numa escala pré-industrial. O tempo de vida da formulação pode aumentar se os HDL forem adicionados num curto espaço de tempo antes da aplicação do revestimento.

Keywords Layered double hydroxide, corrosion, accelerated corrosion test, coating, X-ray diffraction,dispersion, active protection.

Abstract

The main goal of this work is to study the challenges associated to the upscaling of an active protective coating with (LDH) layered double hydroxides from a laboratorial to industrial scale. Two types of coatings having LDH with gluconate intercalated into its galleries with and without alginate as surface modification were considered. Dispersion was studied with both particles in a polymer formulation and it was shown that the addition of alginate allows a faster and more effective dispersion as well as improved compatibility to the matrix. The possible agglomeration of LDH particles in the formulation was evaluated by particle size analysis demonstrating a reasonable compatibility between the pigment and polymer. The developed coatings were studied with standard accelerated corrosion tests and electrochemical techniques demonstrating active protection conferred by the LDH nanocontainers. Coating protection properties were studied through electrochemical impedance spectroscopy and revealed that the addition of LDH allows an active corrosion protection to coatings, higher impedance values and a delay on the appearance of new time constants with the increasing of immersion time. The shelf-life of the LDH pigment as well as LDH-containing coating formulation was estimated by monitoring the crystalline structure of LDH by X-ray diffraction technique. No changes of LDH structure during storage in open air were observed, however, for formulation, there was a change of basal spacing which can be associated to intercalation of anionic species from formulation into LDH galleries.

The obtained results lead to the conclusions that the compatibility of LDH with coating formulation can be improved by modification of pigment particles with alginate when considering pre-industrial scale application. The shelf life of the formulation can be extended if the LDH nanocontainers are added at a later stage shortly before the coating application.

TABLE OF CONTENTS

INDEX OF FIGURES

INDEX OF TABLES

ABBREVIATIONS

GA	Galvannealed
GI	Galvanized
LDH	Layered double hydroxide
LDH-Gluc	Layered double hydroxide with gluconate intercalated
LDH-Alg	LDH-Gluc with alginate as surface modification
LDH-NO_3	Layered double hydroxide with nitrates intercalated
LDH-CO_3	Layered double hydroxide with carbonates intercalated
SST	Salt spray test
ECC1	Cyclic corrosion test
DLS	Dynamic light scattering
SEM	Scanning Electron Microscopy
XRD	X-Ray Diffraction
EDS	Energy-Dispersive x-ray spectroscopy

CHAPTER 1

Introduction

1. Introduction

1.1 Objectives

The main goal of this work is to study the challenges associated to the upscaling of an active protective coating with (LDH) layered double hydroxides from a laboratorial to industrial scale. This thesis was divided with the following objectives in order to achieve the upscalling challenges:

- Study the dispersion of LDH with and without surface modification (alginate) in a polymer formulation
- Study the shelf-life of LDH in open air and in formulation
- Study the performance of obtained active LDH-protective coatings in industrial accelerated corrosion tests such as salt spray test (STT) and Cyclic corrosion tests (ECC1)
- Study the barrier properties of coatings through electrochemical impedance spectroscopy (EIS)
- Study the stability of the LDH in coating formulation through dynamic light scattering (DLS)

1.2 Structure of the Thesis

The thesis consists of 5 chapters. The state of the art will be discussed on chapter 2. It will introduce an idea of the motivation that leads to the aim of this thesis. The experimental part done will be discussed on chapter 3. In Chapter 4, a discussion of results obtained in chapter 3 will be presented. Finally, in Chapter 5, general conclusions and proposed future work are discussed.

CHAPTER 2

State of the Art

2. State of the Art

2.1 Corrosion problem

All the materials used by human kind are exposed to the surrounding environment which often can be reactive. Corrosion is a consequence of the reaction between the metal and corrosive environment which leads to the continuous degradation of the material as time progresses [1]. Corrosion reactions occur because most of the metals are thermodynamically instable when in the presence of different environments such as air, water, acids or other oxidizing agents [2] . Beside metals, corrosion occurs in plastics, concrete, wood, ceramics and composite materials [3].

The severity of a corrosive environment tends to vary significantly with different places. They are historically classified as industrial, urban, marine or rural environment [4]. The industrial environment contains a high content of sulfur dioxides (SO_2) and chlorides (Cl^-) due to the emission of gas pollutants from factories. An urban environment is characterized by the emission of nitrogen oxides (NO_x) and sulfur oxides (SO_x) derived by the emission of gas pollutants from fossil fuels by vehicles. A marine environment is highly corrosive and is characterized by fine chloride salt particles deposited on the metal. Rural environments are the least corrosive ones. This environment does not contain chemical pollutants but contain organic and inorganic particles [5].

Corrosion causes huge losses for humanity, on an economical, environmental and social level. It is estimated that industrialized countries spent 3 to 5 % of their GDP in costs associated to corrosion. The majority of these costs are related to the corrosion damage and the respective maintenance and repairs [6]. Corrosion can lead to catastrophic situations such as the River Queen [7] or the Aloha [6] aircraft incident. Social problems are associated to dismissal of workers due to plant shutdown caused by corrosion [7]. Also environmental consequences can occur due to toxic agent releasing into the nature as a result of corrosive degradation [8].

Corrosion is divided into two main groups: dry and wet. Dry corrosion occurs when there is a reaction between the metal and its environment without any conducting medium; generally it occurs at elevated temperatures [7]. Wet corrosion is associated with electrochemical reactions that happens between metal and moisture (water, condensed moisture and steam) when exposed to the atmosphere, aqueous solution or to the soil.

There are many physical forms taken by wet corrosion with different appearances; they are divided in eight main corrosion forms which can be classified by their visual appearance as uniform or localized. Inside the localized corrosion group, they are divided into two groups being classified as macroscopic or microscopic according to visual appreciation [8]. Figure 1 shows the eight different types of wet corrosion:

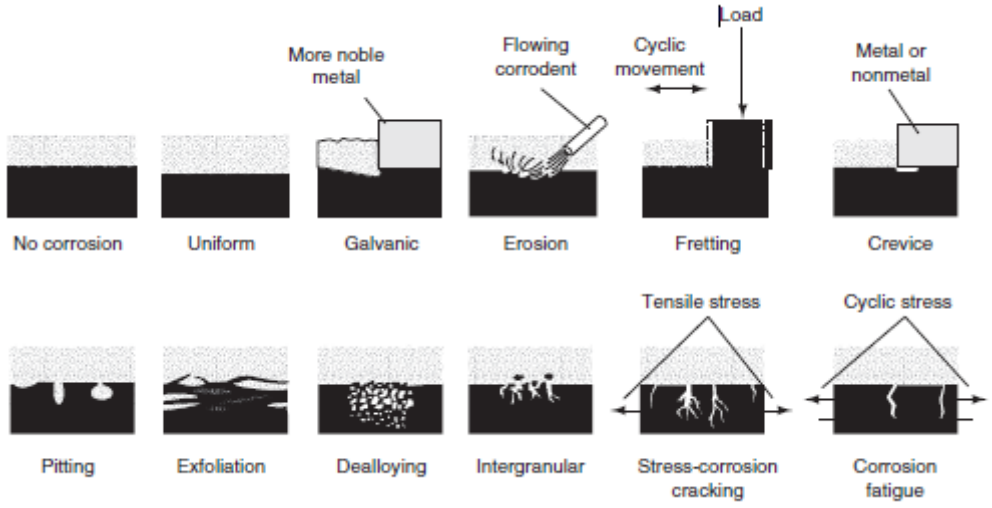

Figure 1- Schematic of wet corrosion forms [8]

When a metal is corroding, corrosion products appear over the metal surface giving an unpleasant aspect, the name given for corrosion products is “rusting”. The rust formed on steel is composed by a hydrated ferric oxide and is red or dark brown [8].

In some metal/environment systems the metal is protected by a natural film formed on the surface. The metal is therefore protected by passivity which decreases its reaction with the corrosive environment. In other systems the passive film is not formed. Therefore metal remains active and some form of protection must be provided [1]. Coatings and protective layers are applied making the metal less sensitive to most environments.

2.2 Protective coatings

Application of protective coatings is one of the most widely used strategies for corrosion control. Coating provides a long-term protection under a variety of corrosive conditions, extending from atmospheric exposure to the most aggressive chemicals [4]. Protective coatings can have a passive corrosion protection, avoiding direct contact of metal with the corrosive medium. Or they can have active corrosion protection with the impregnation of corrosion inhibitors in organic coatings or using metallic coatings, as it will be discussed later.

2.2.1 Metallic coatings

With metallic coatings a layer of metal is created changing surface properties of the metal such as mechanical and physical properties as well corrosion protection. A layer is provided to the metal exhibiting properties generally not achievable by the material when used alone [6]. Coating is attached to the substrate metal and it becomes necessary to have good adhesion with the substrate. Metallic coating can also protect the substrate via sacrificial protection as it occurs with galvanic corrosion between dissimilar metals in contact in a corrosive environment.

The metallic coatings can be applied in different ways, but the most known are electrodeposition and hot dipping [1]. In the case of electrodeposition, a metal is immersed in a tank with the electrolyte containing metal cations which are reduced under cathodic polarization forming a layer on the surface. In a hot-dipping process, metal is immersed in a molten metal bath; metallurgic bonds between the metal (M) and the molten bath component (B) give to the surface a series of distinct M/B alloy. There are several coatings being applied in metals such as aluminium, zinc, tin and others. However one of the most used for steel substrates is zinc [9]. The steels coated with zinc-based layers are called galvanized steels.

2.2.2 Galvanized and galvannealed coatings

The hot dip application of zinc onto steel sheet was developed over 50 years, This process is limited to relatively low melting point coating metals. The most common hot dip coated product is low carbon steel type [10].

In order to produce a galvanic coating, the first step is cleaning the steel to remove oils, soils and other elements in an acid pickling applied for removing scale rust before dipping in the molten zinc [11]. After that, steel is immersed in a bath consisting of a minimum of 98% pure molten zinc with a temperature about 450ºC [12]. During steel immersion, the molten zinc reacts with the iron in the steel forming different layers of zinc/iron alloy. The surface layer has the highest Zn content on the top, as it goes to the inferior layers the content of Fe increases reaching 25% [13].

Zinc is used for corrosion protection due to the excellent corrosion performance of zinc-coated steel in natural environments which corrodes 10 to 100 times slower than steel [14]. Corrosion protection by zinc layer acts in two different ways: the first one is a barrier protection where the zinc coating completely covers the steel surface from the corrosive action of the environment. It is necessary to have a good coating adhesion to the base metal and abrasion resistance in order to maintain coating integrity. The other way to achieve corrosion protection is by galvanic protection by the sacrificial anode method. Zinc is anodic when compared to iron and steel. Hence, zinc corrodes acting as an anode protecting the steel [13].

The alloys formed on bath content in hot dip galvanizing can vary with incorporation of some elements as Al, Cu, Fe and Pb [15]. A new coating was found as having better corrosion protection, this coating is a Zn/Fe which has higher amount of Fe in bath. Galvannealed coating has 8-10% Fe alloy [16]. The key for galvannealed coatings compared with regular galvanized coatings is a decrease of galvanic activity and easier painting which results from a good paint adhesion. In order to produce a galvannealed coating it is necessary to heat the molten coating and steel sheet after the steel sheet is withdrawn from the bath. Steel is heated between 480 – 565ºC during 10 s. During immersion, zinc becomes partially alloyed with the iron from the steel forming layers of Zn/Fe intermetallic compounds. Due higher additions of Fe, the electrochemical potential difference between steel and coating is considerably less compared with to the potential

between galvanized coating and the steel. Therefore the corrosion rate for galvannealed coating is smaller than for galvanized ones [15].

2.2.3 Inorganic coatings

Inorganic coatings also called conversion coatings are produced by chemical action, with or without electrical assistance. This type of coating forms a film of metallic oxide (chromate and anodizing) or compound (phosphate) that has better corrosion resistance than the original metal and provides an effective base for main protection such as paints [4]. There are three main types of inorganic coatings: phosphate, chromate and anodizing coatings and their application varies with the material used, however for steels phosphate ones are used [9].

Phosphate is applied on galvanized, gavannealed and other steels. Likewise it provides good adhesion of the organic coating due to the creation of a stable and adhesive interface between the metallic substrate and the applied paint [17].

2.3 Paints

Paints are introduced as protective layers aiming at formation of a film that creates a physical barrier between the metal and corrosive species. In addition, organic coatings often provide beauty and aesthetical appeal [9]. Normally they are composed by organic binder, pigment and solvents as main components.

2.3.1 Paint components

Paints are pigments dispersed in a solution of a binding media. Binding media is the component that determines the chemical and physical properties of the paint. A coherent continuous network structure is formed after functional groups from structural organic units start to cross-polymerize creating a three-dimensional structure. Alkyd, epoxy, amino and polyurethane resins are some examples of binding medias used in organic coating formulation [4].

Solvents are volatile components of organic coating formulation. They are applied to disperse the binding media and pigments, reduce the viscosity and impart characteristics

needed for applying the paints to the metal surfaces [14]. Different solvents are used in paints such as aliphatic and aromatic hydrocarbons, ketones, esters and alcohols [6].

Pigments are dry powders which are insoluble in the paint medium. Consequently it is needed to mix them with a dispersion technique [6]. These components are added to the paint in order to give the desired color and anti-corrosion protection with the impregnation of corrosion inhibitors. Extenders are compounds used to replace part of the pigment content to reduce costs [14].

2.4 Corrosion inhibitors

The addition of inhibitors to the paint can control or reduce the corrosion of metallic surfaces due to the formation of a protective film on the surface metal. A corrosion inhibitor is a chemical compound that when added to a solution in small amounts leads to a decreasing of corrosion rate [15].

There is no an agreement in the literature about inhibitor classification. According to McCafferty [3], inhibitors are classified in two main types: (i) adsorption inhibitors and (ii) film-forming inhibitors. The second type can be divided into two sub-groups as passivating (i) or precipitation inhibitors (ii). Jones [16] classified inhibitors by their chemical functionality as inorganic inhibitors, organic cationic and anionic. Roberge [4] classifies corrosion inhibitors in a functionally scheme as anodic, organic, precipitation inhibitors and volatile corrosion inhibitors.

Passivating or anodic inhibitors cause a large anodic shift of the corrosion potential, forcing the metallic surface to become passive. There are two types of anodic inhibitiors, according to the presence of oxygen (oxidizing) or not (nonoxidizing) [16]. Cathodic or precipitation inhibitors allow a delay of the cathodic reactions or selective precipitation of insoluble compounds on cathodic areas. The formation of insoluble compound avoids the diffusion of corrosion species to these areas [4]. Organic inhibitors protect the metal by forming a film on the metal interface due its chemisorptions. Its network keeps the water molecules and aggressive anions such as Cl^- away from the metal surface [4]. Vapor phase inhibitors (VPIs) are compounds with low vapor pressures that when in a closed system, they volatilize and the vapor condenses on the metal surface to provide protection. These inhibitors are widely used in boilers [16].

There is a wide variety of inhibitors applied to metals, the most widely anodic inhibitors for oxidizing anions are chromates, nitrates and nitrites whereas from nonoxidizing ions are phosphate, tungstate, and molybdate [16]. The most used cathodic inhibitors are arsenic, antimony and bismuth. Whereas the most common organic inhibitors are amines, imines, thiourea, mercaptans, guandine and aldehydes [15].

The most widely used inhibitor applied on galvanized steel are chromates but this compound is toxic for the humans and its utilization is limited just for some applications such as aeronautical industry [4].

2.5 Anticorrosive polymer coatings

A substrate in real situations has a complex system approach that provides an excellent answer for many specific coatings requirements. Anticorrosive coating is a complex system that has several layers with specific roles.

In many cases a coating system is composed by primer, intermediate coats and a top coat. The main function of primer is to provide strong adhesion to the substrate as well as corrosion and chemical resistance. Primer is the base upon which the rest of the coating system is applied. Intermediate coats are used in order to provide a superior barrier with respect to aggressive chemicals from the environment and strong adhesion to the primer and the top coat. Finally the last layer of an anticorrosive coating is the top coat, this layer´s function is to provide a resistant seal for the corrosion system, form the first barrier against the environment and provide a pleasing appearance to the coating [18].

2.5.1 “Self-healing” concept and new approaches

Coatings are exposed to the surrounding environment and can start to degrade due to the action of UV radiation, mechanical action, temperatures gradients and mechanical stresses [19]. Aggressive species diffuse and propagate through the coating reacting with the substrate leading to a faster development of the defects. In this way, a “self-healing” of defects in the coating and on the metal surface is desirable when aiming at long term protection.

The term “self-healing” is associated with the ability of a material recover its initial properties after destructive forces coming from an external environment and the influence of internal stresses. In nature, “self-healing” means a complete recovery of the coating due to a real healing of the defect, restoring the initial coating integrity. “Self-healing” for anticorrosion coatings is achieved when active species are incorporated. Thus, the corrosion activity is hindered in defect and on the substrate due to the action of active species. In anticorrosion coatings a complete recovery of all coating properties is not expected; merely a protective action against corrosion [20].

There are several studies found in literature in order to achieve “self-healing” behavior by anticorrosive coatings with different strategies and systems. Coating with a self-healing ability was studied based on the reflow effect. These coatings are based on the polymerization of a healing agent in the defects. The barrier properties of the protective coatings are recovered [21]. Another point of view to achieve a “self-healing” effect in protective coatings is based on a simple blocking of the defects with insoluble precipitates. Defects are blocked due to the formation of corrosion products when reacted with the corrosive medium [22]. Both strategies mentioned above create a real healing effect on defects which partially recovered the physical integrity of the coating. However, an effective hindering of corrosion is not achieved by a blocking of the pathways for corrosive species. The main function of a protective coating is to protect the substrate against the corrosion processes. Corrosion processes can occur under the coating where the electrolyte has already penetrated into the substrate when the defect was induced. Some strategies were developed in order to achieve active corrosion protection in defected areas where corrosion processes take place [23].

Electroactive condutive polymers (CPs) are currently being studied in coatings as possible environmental-friendly systems. The metal is anodic polarized by CPs in the presence of an electrolyte. Thus, a shift of the metal potential into the passivity region leads to a formation of a passive film. This shift is caused by the anodic protection by CPs which decreases drastically the corrosion current. Polyanilines, polyheterocycles and poly(phenylene vinylenes) are the polymers used in CPs coatings. An active anticorrosion protection and “self-healing” effect is achieved by CPs [24]. However, these CPs systems are not used in real industrial applications. Coatings used for industrial applications must meet many requirements such as: high chemical stability when coming into contact with

air and water, good compatibility with a conventional organic paint system, good adhesion on the metal and on the topcoats [23].

Utilization of chemical inhibiting species are another approach for active corrosion protection and a self-healing effect aiming at hindering corrosion activity. The inhibitors can be incorporated in the different layers of coating system. Conversion coatings such as phosphates have inhibiting behavior. An inorganic crystalline layer is formed on the surface which is less reactive to subsequent corrosion than the original metal surface. The most effective conversion coatings are chromate based [20]. Because it is strongly carcinogenic new conversion coatings with self-healing effect have been studied for their incorporation of inorganic and organic corrosion inhibitors.

Another way to achieve active corrosion protection with a self-healing effect is the introduction of inhibitors in the coating matrix. The introduction of a corrosion inhibitor in the matrix occurs with just a simple mixing with a coating formulation. However, it is difficult to introduce inhibitors because some important factors should be considered [23]. The inhibition is effective if the solubility in the coating matrix is in the right range. If the inhibitors have a very low solubility, there is a weak self-healing effect due to a lack of active agent at the substrate interface. If the solubility is too high, the substrate is protected but just for a short time. This is due to the fact that the inhibitor will be rapidly leached out from the coating. Also, too high solubility creates osmotic pressures that forces water permeation. Water permeation leads to blistering and delamination of the protective coating [25]. Degradation of the barrier properties due to chemical interactions between inhibitor and coating components is the main issue with the development of active corrosion protection systems.

The incorporation of corrosion inhibitors in the matrix were studied in multiple ways, since the use of sol-gel films to metallic alloys films. It was proven that the direct addiction of corrosion inhibitors in some case confers additional active corrosion protection and self-healing abilities. However, very often inhibitors react with the polymer causing the weakening of the barrier properties and therefore overall corrosion protection. Thus, strategies have been developed to immobilize inhibitors in nanocontainers when incorporated in the polymer matrix [20].

2.6 "Smart" self healing coatings with nanocontainers

The study of new active anti corrosion coatings based on corrosion inhibitors in nanocontainers started in the early 2000´s. Corrosion inhibitors are introduced in "host active" structures and are released when in the presence of corrosion activity. As a result, a uniform distribution of nanocontainers in the matrix is achieved with the active species remaining in a trapped state. The problem that occurs when inhibitors are freely distributed in the matrix is thereby minimized. The obtained results show considerable improvement of the corrosion resistance. New approaches based on the encapsulation of inhibiting compounds before addition to the coating system have been suggested over last years.

2.6.1 Types of nanocontainers

There are several nanocontainers applied for active corrosion protection coatings. They can be oxide nanoparticles, porous nanostructured layers, LbL constructed nanocontainers, halloysites nanocontainers or LDH nanocontainers. The mechanism of inhibitor release varies according to the type of nanocontainers used [20].

Lamaka et al [26] studied nanoporous titania interlayers as a reservoir of corrosion inhibitors for active corrosion protection. The study's aim was to find new environmental-friendly primers for AA2024-T3 alloy using a sol-gel matrix. Inhibitors were immobilized between TiO_2 and sol-gel film. The system showed enhanced corrosion protection and a self-healing ability. Another strategy used for immobilization of inhibitors in nanocontainers employing oxide nanoparticles. The addition of oxide nanoparticles allows enhanced barrier properties reinforcing the coating formulations [27]. Inhibitors cations such as Ce^{3+} were immobilized in amorphous ZrO_2 nanoparticles [28]. The corrosion resistance of phosphatised organic coatings with rare earth nanoparticles was studied on 6061-T6 aluminium alloy [29]. The addition of different rare-earth oxide nanoparticles has influence in the coating resistance. A different strategy used to provide active corrosion protection to coatings is using local pH changes in anodic and cathodic sites as triggered. A way to achieve inhibitor control release is coating inorganic nanocontainers using layer-by-layer (LbL) technique. Nanocontainers are coated layer by layer with polyelectrolyte shells. Benzotriazole was incorporated as corrosion inhibitor between oppositely charged polyelectrolyte layers [30]. In this way, layer upon layer of the various polyelectrolytes are

formed. SiO_2 nanoparticles were firstly coated with a layer of positively charged poly(ethylene sulfonate) (PES) followed by adsorption of negatively charged poly(styrene sulfonate) (PSS) and then with positively charge benzotriazole. Falcon et al also studied nanocontainers by LbL technique with the same process but with a different inhibitor (dodecylamine) [31]. Natural halloysites nanotubes were also coated with polyelectrolyte shells by LbL technique. These nanotubes confer a higher loading capacity of the corrosion inhibitor when compared with SiO_2 nanoparticles. Halloysites were coated with poly(allyalimine hydrocholoride) (PAH) and PSS whereas 2-mercaptobenzothiazole was used as corrosion inhibitor [32]. It was observed that is not possible to achieve an inhibitor release control of active species.

Coatings are subjected to degradation due to external factors such as UV radiation, temperature and mechanical action [33]. When corrosion processes start in the defect, nanocontainers respond by releasing the immobilized inhibitor locally. Cathodic and anodic reactions occur between the inhibitor and the metal forming a protective passive film (Figure 2). Using a system that encapsulates the inhibitor, the negative effect of the inhibitor is reduced, inhibitor deactivation due to interaction with the coating components is prevented and therefore there is a controllable release of the inhibitor on demand [23].

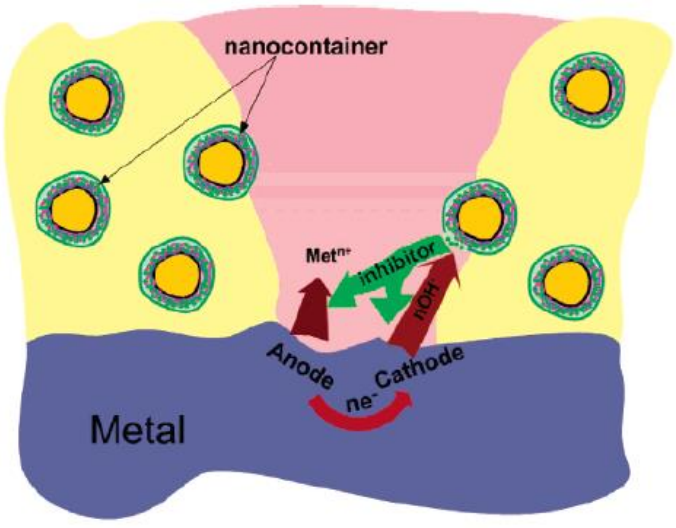

Figure 2 Schematic mechanism representation of active protective coatings with nanocontainers [25]

A more complex system is based on the release of inhibitor by ion-exchange. Two types of nanocontainers are used in ion-exchange control release. The first one is Layered Double Hydroxide (LDH) that will be discussed with more detail further and the second is bentonite. Bentonite is a cation-exchanger. This nanocontainer consists of stacks of negatively charged aluminosilicate sheets, where inhibiting cations are intercalated between them [34]. Bentonites present anticorrosion behavior when doped with inhibitor, however, some problems were found because cations may not be directly associated with corrosion processes, which can lead to a waste of inhibitor [40].

The importance of nanocontainer dispersion in organic matrices for industrial applications is still in its infancy stage. The potential use of nanocontainers on an industrial scale varies according to its type. Although nanocontainers coated with polyelectrolyte shells by LbL technique are interesting due to pH-triggered mechanism, their scale up is limited due to the methodology of LbL. For LDHs, the scale up of synthesis is cost-effective and feasible [33].

2.7 Layered Double Hydroxides

LDHs are present in nature as hydrotalcite ($[Mg_6Al_2(OH)_6CO_3.4H_2O]$) and pyoaurite ($[Mg_6Fe_2CO_3(OH)_{16}.4H_2O]$) being known for over 150 years.

LDHs have a host-guest structure [35] by galleries where anionic species and solvent molecules can be intercalated. The galleries are surrounding by crystalline inorganic structures consisting of stacks of positively-charged mixed-metal hydroxides (Fig.3). The reason for why anionic and solvent species molecules are intercalated is because LDH structure is based on the brucite [$Mg(OH)_2$] structure [36]. Divalent cations are substituted by trivalent ones, with the layers of hydroxide becoming positively charged. The presence of negatively charged anions and water molecules within the interlayer space compensate the charge and stabilize the LDH structure.

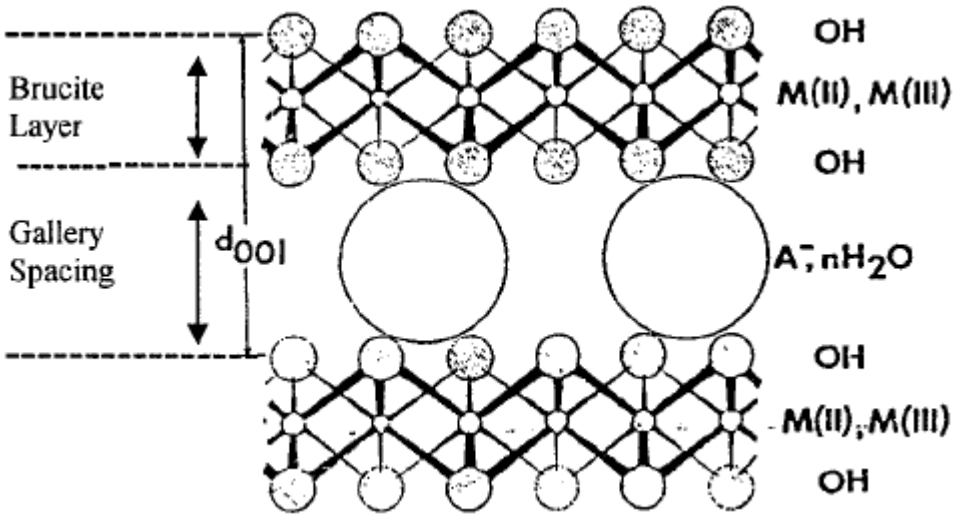

Figure 3 Host guest structure of LDH [38]

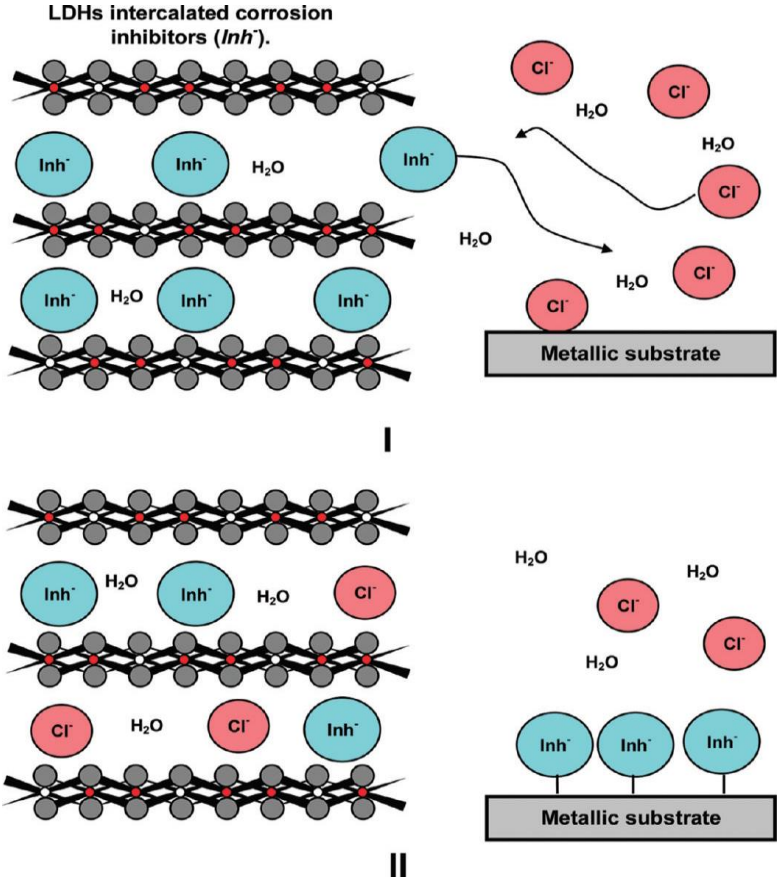

Figure 4 Mechanism of anion-exchange by LDH [19]

When in presence of aggressive species such as chlorides LDH plays a double role in active corrosion protection. The first role can be observed as I in Figure 4. When in high concentration of Cl^-, intercalated inhibitors are released from LDH forming a passive film

and the metallic substrate is protected (II). At the same time, Cl^- and other anionic species are entrapped in the LDH galleries decreasing the presence aggressive of species in the coating [19]. Besides the anion-exchange in presence of anionic species, the release of inhibitors can be indirectly triggered by pH changes. Hydroxyl anions at high pH can be exchanged with the inhibitors while at low pH the LDHs dissolved releasing the entrapped inhibitors [33].

Layered double hydroxide can be synthesized. The first one to make synthetic LDH was Feitknecht in 1942. Since then, its structural characterization has only started in the 60´s [36]. There are different routes for synthetic preparation of LDHs including co-precipitation, ion-exchange and calcinations-rehydration methods. Due to its versatile structure LDH can allocate either different inorganic [19, 37, 39] or organic anions [19, 40, 41].

LDHs have been studied by different groups as containers for corrosion inhibitors [19]. There are several works published in scientific literature about LDH as a possible nanocontainer for active and controllable corrosion protection. Buchheit and his colleagues are one of the pioneers for the utilization of LDHs intercalated with corrosion inhibitors [39]. During this work Zn-Al LDHs containing vanadates in decavanate form were dispersed in an amide-cured bisphenol epoxy resin and tested over a coated aluminum alloy. The active corrosion protection was tested. It was concluded that the worst results were obtained with the blank coatings. Nonetheless, the best results were obtained by coatings with LDH-vanadates. Tedim et al studied Zn-Al LDHs intercalated with nitrate anions as chloride nanotraps for organic polymeric coatings [42]. The addition of such nanotraps to a polymer layer drastically reduces the permeability of corrosive anions through the protective coatings. A study was made about the controllable release of divanadate anions in Mg-Al and Zn-Al hydroxides structures over an aluminium alloy 2024 as substrate [37]. Zn-Al LDH-nanocontainers provide a well-defined self-healing effect. Organic and inorganic inhibitors (vanadate, phosphate and 2-mercaptobenzothiazolete) were incorporated in LDHs and applied on alloy AA2024 [19]. Active protection was enhanced when protective coating system is combined with LDH is loaded with different inhibitors. Montemor et al studied the incorporation into the coating system (epoxy based coating) of LDH and cerium molybdate hollow nanocontainers both loaded with 2-mercaptobenzotriazole as corrosion inhibitor [41]. The coating was applied

over GI steel. The results showed that the combination of both nanocontainers in coating system provides corrosion inhibition and self-healing effect.

LDHs in order to be effective in active corrosive dispersion should be well dispersed in the matrix. Coating barrier properties are affected when agglomerates of LDH are formed [19]. Therefore it has been studied the modification of LDH surface for a better dispersion.

2.7.1 Surface modification

Nanoparticles have strong tendency to agglomerate due to high surface. Modifying its surface with polymer or a surfactant is a strategy to improve stability inducing strong repulsion between nanopartarticles. Therefore the dispersion becomes easier [43].

Alginate is a promising polymer for surface modification of nanoparticles. Alginate is an anionic polysaccharide and is composed by β-D-mannuronate (M) and α-L-guluronate (G) units where different M/G ratios can vary depending on origin [44] (Figure 5).

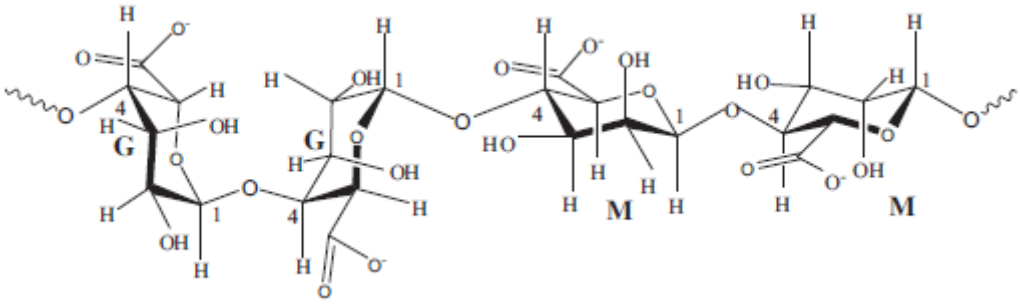

Figure 5 Structure of alginate [44]

Because it is negatively charged, alginate allows a good compatibility with the positively charged LDH surface.

2.8 Upscaling challenges

To date, there is no data in the relevant literature on the application of active protective coatings with LDHs over galvannealed layer. Also the challenges faced on the application of “smart” coatings on an industrial scale as shelf-life of nanocontainers in coatings formulations has not yet been observed.

CHAPTER 3

Experimental Procedure

3. Experimental Procedure

The experimental part of this work is divided in two parts. One is related to the experiments performed in the university lab and second one associated to the results obtained at industrial laboratory. Coatings were tested in salt spray test (SST), "*essai de corrosion cyclique"* (ECC1) and electrochemical impedance spectroscopy (EIS). A GA substrate was coated by a commercial polymer amino imine formulation (PXM 10174) which was used as primer. Corrosion inhibitor (gluconate) was intercalated in layer double hydroxides (LDH). LDH were dispersed in the formulation in order to achieve active corrosion protection. The obtained LDH intercalated with gluconate were dispersed with surface modification (LDH-Alg) and without surface medication (LDH-Gluc)

3.1 LDH synthesis by co-precipitation method

The LDH used during this work were Zn-Al structure. LDH-NO_3 was obtained by co-precipitation method of hydroxides formed from Zn and Al nitrates salts into a $NaNO_3$ solution at constant pH and under nitrogen atmosphere. In order to avoid contamination with carbonate anions, all the solutions were prepared using boiled distilled water. A 0.5 M $Zn(NO_3)_2.6H_2O$ and 0.25M $Al(NO_3)_3$ in 50 ml solution was slowly added to 1,5M $NaNO_3$ (V=100ml and pH 10) under vigorous stirring at room temperature during roughly 1,5 hours, being the pH kept constant by simultaneous addition of 2M NaOH. A hydrothermal treatment was done with the following conditions: 100ºC during 4h, centrifuged and washed four times with distilled boiled water and dried at 60ºC during 24h was made to the obtained slurry for LDH crystallization. [42]

3.2 LDH intercalation

LDH-Gluc was obtained by anion-exchange using LDH-NO_3 as starting material. LDH-NO_3 was added to a first portion of 0.1M sodium gluconate and maintained under constant stirring for 24 h. The reaction product was then centrifuged (10000rpm during 4 minutes) and washed three times with boiled distilled water for nitrate removal.

Subsequently, a second portion of sodium gluconate solution was added to the precipitate and the anion-exchange procedure repeated. Finally, the gluconate-loaded LDHs were washed and centrifuged three times with boiled distilled water, and dried at 60ºC during roughly 24h. The same process was used for intercalation of carbonates in LDH but a solution 0.1M of sodium carbonate was employed in this case.

3.3 LDH functionalization

LDH-Alg was obtained by constant stirring 80ml dispersion containing nanoparticles (0.4g) and 20ml solution of alginate (0.5%wt). The pH remained constant (pH 5) for dissolution of alginate during 15 minutes at room temperature. After stirring, the solution was centrifuged and washed with distilled water three times to ensure that all alginate in excess was removed.

3.4 Dispersion of LDH

Coating formulation was prepared for later application over the substrate. The coating formulation is composed by LDH-Gluc or LDH-Alg dispersed in a commercial PXM 10174 polymer formulation. LDH particles were dispersed mainly by mechanical stirring in a magnetic plate with controllable velocity in industry. Firstly 10g of polymer formulation were added with the desire amount of particles and stirred. After that, an ultrasonic bath to improve dispersion was applied. Magnetic stirring and ultrasound were applied multiple times as shown in Figure 6. When totally dispersed, another 10g of polymer formulation were added and repeated the same process. Dispersion occurred at room temperature with velocities varying between 1500 and 1700 rpm. The different steps and times for dispersion in industry are observed in Figure 6. Also ultra velocity dispersor (Turex) was used for dispersion of LDH in the polymer formulation.

.

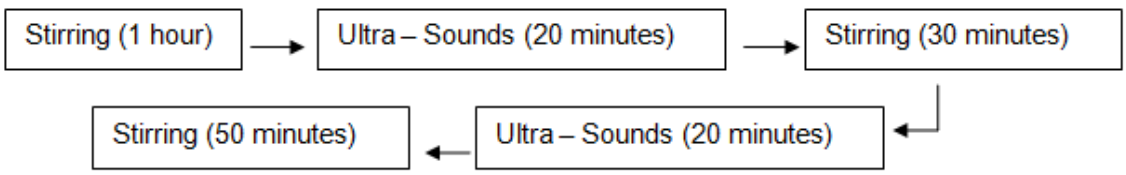

Figure 6 Diagram of dispersion

In laboratory, the dispersion was performed with a Turex with velocities around 10000rpm. Dispersion took 4 minutes and after that ultrasonic agitation was applied during 3 minutes to further increase the particles dispersability.

The amount of LDH used in the coating, was chosen according to the percentage of LDH in the matrix after cured the sample. Table 1 presents the conditions used in industry and laboratory:

Table 1 Concentrations and systems used during this work

Environment	System	Concentration (%wt)	Dispersion Mechanism
Industry	LDH-Alg	2,5	Magnetic Stirring
		5	
		10	
		10	Turex
	LDH-Gluc	2,5	Magnetic Stirring
		5	
Laboratory	LDH-Gluc	1	Turex
		2,5	
		5	
		7,5	
		10	
		20	

3.5 XRD analyses

The crystalline structure of the shelf-life of the LDH-coating formulation as well as shelf-life of the LDH pigments was studied by X-ray diffraction (XRD). This study aim understand if long-term storage has an effect on the crystalline structure of LDH and if any changes happen with intercalated anions.

XRD is an analytical technique used for phase identification of a crystalline material and it provides information of unit cell dimensions. The crystalline structure act as a three-dimensional diffraction for X-ray wavelengths similar to the spacing planes in a crystal lattice [45]. X-rays are produced by a cathode ray tube and are emitted directed toward the sample. The interaction between x-rays and sample produces constructive interfaces and a diffracted ray when conditions satisfy Bragg´s Law. The wavelength of electromagnetic radiation to the diffraction angle and the lattice spacing in a crystalline structure are related in this law. The diffracted rays are collected by X-ray detector [46].

LDH-slurry was dried in an oven at 60ºC during 24 hours and then milled with a pestle and mortar. XRD data were collected at room temperature using a Philips X´Pert MPD diffractometer (Bragg-Brentano geometry, Cu Kα radiation, tube power 45°kV, 40°mA, PIXel detector) over the angular range $3.5<2\theta<65°$). For the low-angle measurements ($1<2\theta<10°$) a beam knife was used.

3.6 Particle size

Dynamic light scattering (DLS) allows determining the size of nanoparticles in solution. DLS measures the intensity of light scattered by particles in the suspension as a function of time. Due to Brownian motion of particles in suspension, a change in light intensity is collected by detectors. By measuring the time scale of light intensity fluctuations, the size distribution of particles can be measured [45].

The particle size of LDH-pigment in different concentrations was determined using DLS technique. These measurements aim to verify if any LDH-agglomeration occurred in the paint formulation. DLS measurements were performed on Malvern ZetaSizer Nanoseries. Preparation of the samples for measurement was carried out according to the specifications [47]

3.7 Coating application

Before application the substrates were cleaned. GA steel was provided by TATA Steel Ijmuiden and was received as metal sheets; these sheets were cut and substrate was obtained with a specific size. The size of industrial samples (10 x 15cm) was larger than that of laboratorial ones (4 x 8 cm). Two requirements are necessary for the substrate: they should be as flat as possible and the edges should not stick during cuts.

After the cut, samples were cleaned in an alkaline solution (1,5 – 2.5%wt) in a glass beaker with enough volume to immerse the sample. Alkaline solution was under constant stirring (~400 rpm) at temperature of 58-59°C conditions. The immersion of GA samples occurred during 45 – 60 seconds under constant stirring. After immersion, the samples were washed with deionised water and brushed aiming at removal of dust or grease remaining on the surface. During washing, it was observed if any contamination remained on the surface. A water wetting test was used to check cleanliness of the surface. In the case of well cleaned substrate the water forms a uniform film over the entire surface. When any contamination remains, it is created patches when water passes through the surface, the washing process is repeated until this effect disappears. After washing, the substrate was dried with a pressurized air.

Samples were coated using two methods: in the industry a wirebar was used whereas in the laboratory samples were coated with a bar-coater (Figure 7).

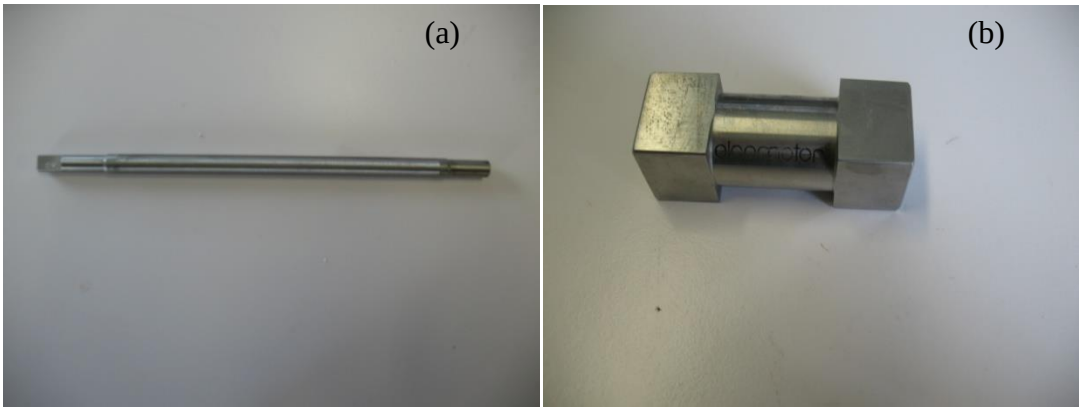

Figure 7 Coater used in: (a) Industry and (b) laboratory

Coating formulation was applied on sample extremity with the coater pushing the formulation throughout the surface. In the industrial sample, an automatic coater was used

with uniform velocity (50 $mm.s^{-1}$) and pressure, in the laboratory the formulation was applied manually.

The obtained sample in the industry had its surface completely coated whereas in the laboratory samples just a stripe with 2 cm of coating was applied on the sample.

3.8 Curing process

The samples with applied coating formulation were cured in order to form a stable polymer network on the surface. The curing process was done in two steps, involving different temperatures. The first stage is a pre-curing at 100°C during 3 minutes in an oven. It is needed because water must be released from the coating formulation. The second step is curing the coating in a convection furnace. This step involves temperature of 265°C during 8 minutes. After the curing, sample was immediately immersed in deionised water and then dried by pressurized air.

3.9 Sample preparation for corrosion accelerated tests

A grey non reactive tape was placed around the sample and when fixed, with a knife a smooth continuous defect was made over the surface. The defect was made with a gap of 1 cm to the edges of the coated surface.

3.10 Industrial accelerated corrosion test

Coated samples were submitted to industrial accelerated corrosion tests. These tests allow understanding the behavior of coated samples under certain corrosive conditions. Two tests were performed during this work: under static and cyclic emission of corrosive specimens.

Salt spray test (SST) was the static corrosion test used, it was performed according ASTM norm B111-73[48]. These standards describes the necessary information to carry out such as temperature (35°C), preparation of spraying solution (5% NaCl) and pH (~3). SST occurred in a close chamber with continuously spraying nozzle during 500 hours.

Cyclic corrosion tests (ECC1) was the cyclic corrosion tested [49]. During the experiment, 1% NaCl at a pH 4 was vaporized during 0.5h in a close chamber cyclically. During the exposure time the relative humidity (%) and temperature (°C) varies (Figure 8). The running time of ECC1 in this work was 10 weeks.

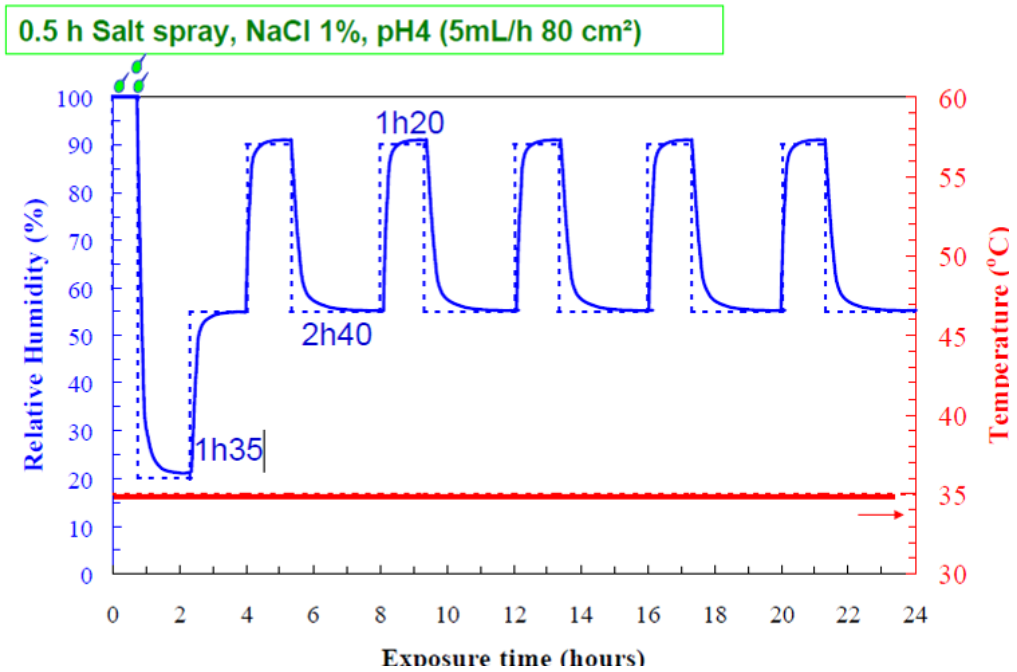

Figure 8 Conditions used in ECC1 test

3.11 Microscopic characterization

Samples were microscopically characterized by optical and scanning electronic microscopy (SEM). The instrument used for optical characterization was Olympus BX51M with magnification 5, 10, 20, 50 and 100 times. Leo 438 VP coupled with energy dispersive spectroscopy (EDS) and Carl-Zeiss AG-Ultra 55 was used for SEM experiments. A thin layer of carbon was deposited on the surface of samples before SEM in order to ensure conductivity and decrease surface charging.

SEM obtains images with high resolution of the sample surface with three-dimensional appearance. High energy beam of electrons for imaging and analysis are produced in high vacuum. The image obtained is dependent with the specimen used. The specimen should be sufficiently electrically conductive to ensure that the bulk of incoming electrons goes to ground. Chemical information of specimen can be obtained by SEM

using X-ray energy dispersive (EDS). This characterization is due to the interaction of some source of x-ray excitation and the sample [50].

3.12 EIS measurements

Electrochemical impedance spectroscopy (EIS) is a non-destructive technique and it provides information about the properties but also processes as corrosion passing the time. This technique allows distinguishing the electric and dielectric properties of individual contributions of components under investigation.

Besides none-destructive and time dependent technique EIS allows useful information for coatings. The deterioration of the coating and consequent corrosion rate of the underlying substrate can be measured by EIS. Moreover, EIS provides information of the electrochemical reaction in terms of resistance and capacitance. Resistance occurs due to electron transfer reaction such as corrosion. Capacitance is associated to changes in the coating due deteoration due to water permeability and porosity in the coating [51].

EIS measurement were carried out on the coated samples at room temperature in a three-electrode cell consisting of a saturated calomel reference electrode, a platinum electrode and the coated samples was working electrode in the horizontal position (exposed are of $3cm^2$). The cell was placed in a Faraday cage to avoid the interference with external electromagnetic fields. The electrolyte was 0.5M NaCl aqueous solution (10mL), stagnant and in equilibrium with air. The measurements were performed using a Gamry FAS2 Femtostat. The selected frequency range was from 0.01 to 10^5 Hz. All the spectra were recorded at open circuit potential.

CHAPTER 4

Results and Discussion

4. Results and Discussion

4.1 Coating preparation and basic characterization

4.1.1 Dispersion

Dispersion of particles is a fundamental step in order to ensure good barrier properties for coatings. Two different dispersion approaches were used: one at industrial scale (TATA Steel lab) and another one at laboratory scale. In industrial lab LDH-Gluc and LDH-Alg were dispersed in the polymer formulation by a magnetic stirring. In laboratory, the dispersion was obtained by mixing LDH-Gluc in the polymer by ultra-high velocity dispersor (Turex). Dispersion in laboratory was achieved after four minutes of stirring with high rotation speed (10000 rpm) and three minutes in an ultrasonic bath.

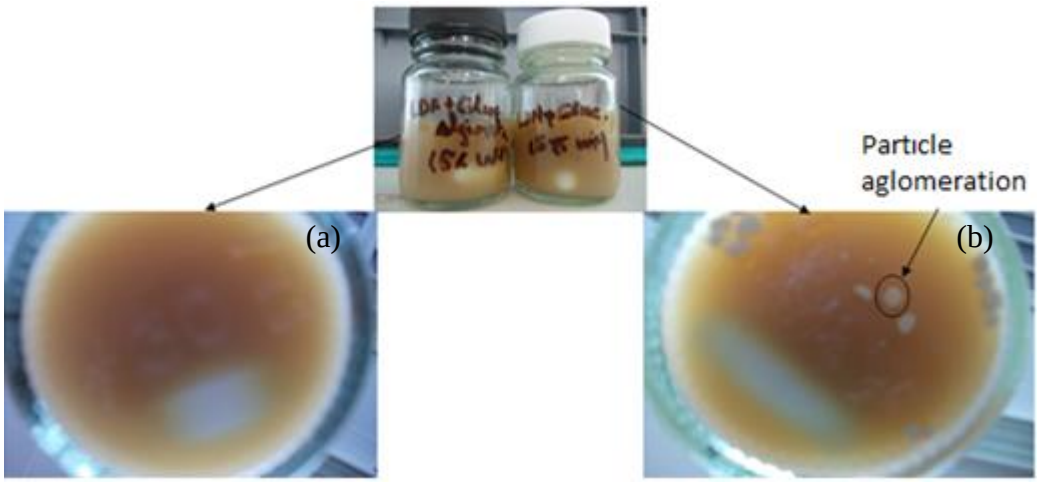

Figure 9 Dispersion of LDH (5%wt) for: LDH-Alg (a) and LDH-Gluc (b) in industry

It was observed that the dispersion time of the particles in industry was different for different particles added (LDH-Gluc and LDH-Alg). For LDH-Alg the dispersion was faster and more efficient comparing to LDH-Gluc (Figure 8). Dispersion efficiency here is reciprocal to time needed for the complete dispersion of LDH. This efficiency results from the strong interactions between the hydroxyl and carboxyl groups along alginate chains and

the positively charged surface of LDH that stabilize the LDH in the water based polymer formulation [70].

In industry the dispersion was done by using mechanical stirring and ultrasonic agitation. Besides the addition of particles with and without surface modification, the dispersion using different concentrations were tested. The longest dispersion was roughly 3 hours for smallest concentrations. So, as LDH concentration increases, the dispersion time decreased substantially (~ 40 minutes) for both type of LDH. Dispersion with higher LDH concentration should be faster due to higher concentration of water and LDH for the same volume that increases shear forces.

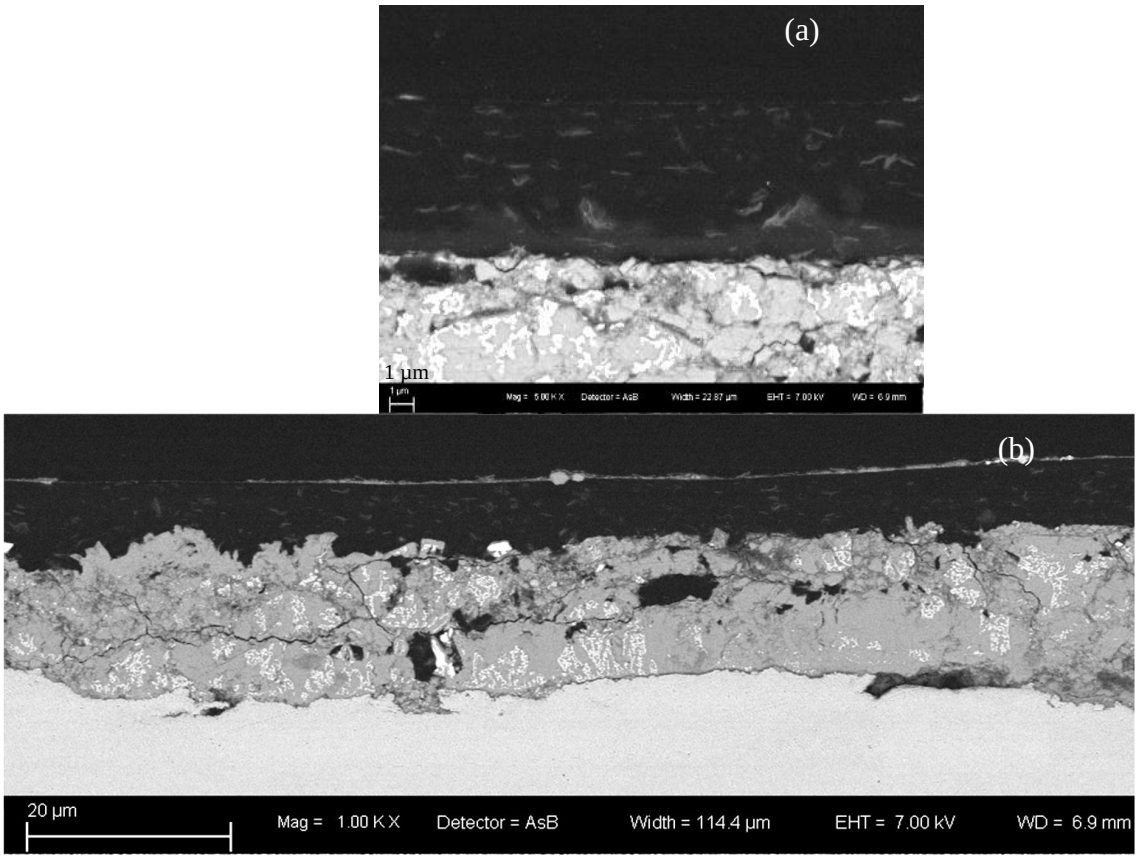

Figure 10 SEM micrograph of dispersed LDH in the coating: (a) LDH-Alg and (b) LDH-Gluc

Alginate not only allows a faster and efficient dispersion of LDH but also allows good dispersion in the polymer after curing. Image (a) of Figure 10 shows that LDH platelets are preferentially ordered in parallel way to GA layer, whereas, the dispersed LDH in image (b) is not so ordered. For both images there are no sign of LDH agglomeration.

Because LDH-Alg is well ordered in the coating, it can have a positive effect on corrosion protection due to higher physical barrier provided against corrosive species.

4.2 Coating application

Coating formulation was applied following different approaches, one for industry and another for laboratory. For industrial samples, coating application was performed automatically with the wirebar covering the entire sample surface. In laboratory the coating was applied manually and had a width of 2 cm and a length of 8 cm. The sample should be as flat as possible in order to avoid differences in coating thickness and defects such as incomplete coverage with the formulation.

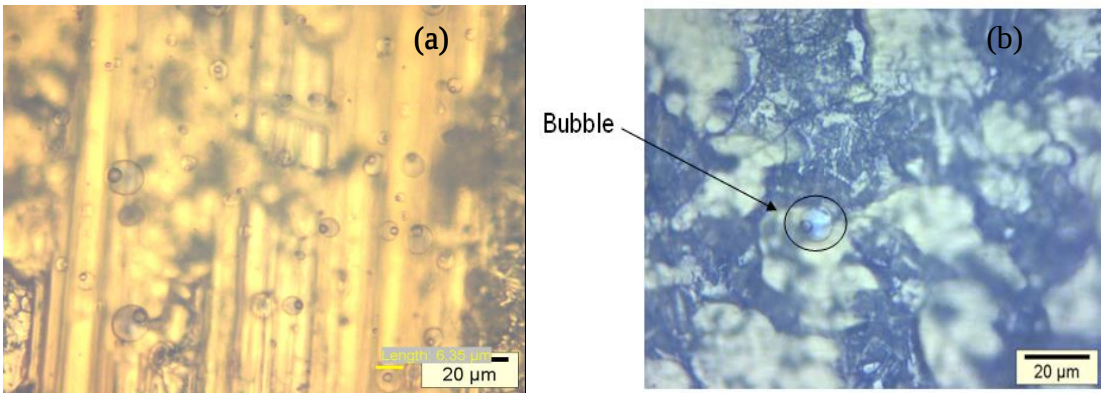

Figure 11 Micro-bubble defects (a) before and (b) after removing anti-foaming additive

Optical microscopy was carried out to verify if any possible micro defects are present in the coating. The first formulation used had industrial anti-foaming additive. This component reduces formation of foam during the industrial processes. Image (a) of Figure 11 shows the resulting coating with anti-foaming additive. The layer was full of micro-bubbles with roughly 7 µm of diameter. Microscopic images of control and LDH coatings were analysed in order to verify if these micro-bubbles resulted from the addition of LDH to the polymer formulation. However, there was no difference between them. Thus, it was removed the anti-foaming agent, and the microscopic images of new coating (Figure 11-b) shows a substantial decrease in the amount of micro-bubbles. Formation of micro-bubbles decreases coating corrosion protection; they appear as empty space with depth in the coatings, creating areas for diffusion of water and aggressive species through coating.

When comparing laboratory and industrial scale some challenges appear. Because more surfaces are coated in an industrial scale the probability of defects is higher. These defects can appear as a result of fixation of impurities and dust from the environment during coating application. The problem observed when samples are not completely flat can be solved applying a rolling system. Therefore as the coating is applied and the sample passes through the rolling, samples becomes flat.

4.3 Particle size analysis

The agglomeration of the pigments in paint formulations is a typical problem which can lead to lower barrier properties. In the present study the LDH particle size distribution in the coating formulation was investigated as function of concentration of the pigment.

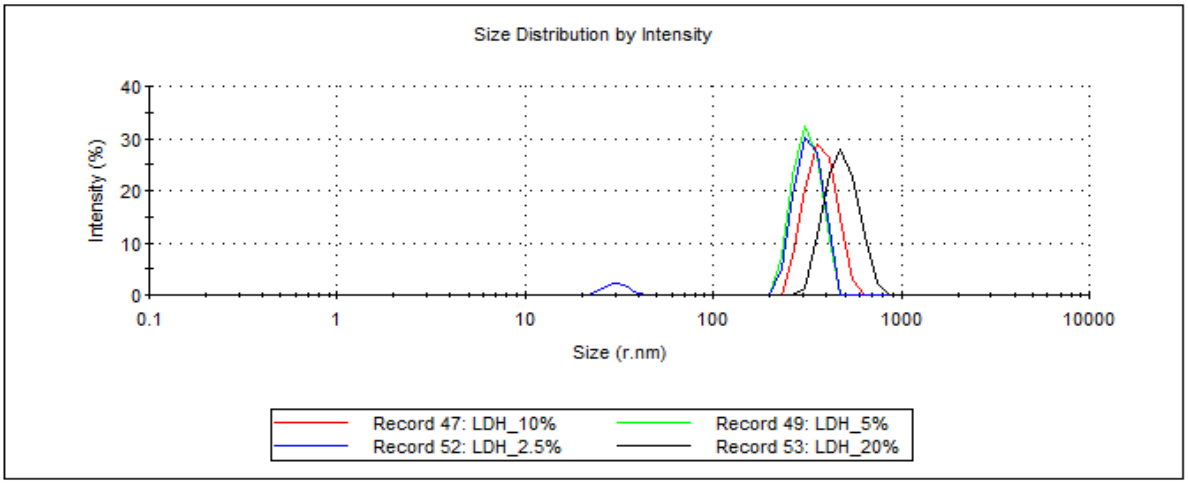

Figure 12 Particle size distribution for LDH-Gluc formulation

The results of particle size measurements show that the average effective diameter of LDH particles varies in the range from 200 nm to 600 nm (Figure 12). A clear trend can be observed demonstarting increase of the average particle size when concentration of the pigment increases. The increase of the size can be related to the fact that dispersed LDH particles form strongly linked agregates of the single flakes. The size of the agregates is a function of the concentration of the suspension. Formation of larger particles can certainly be important for the colloidal stability of the system. However such aggreagates can not be considered as just physical aglomerates. There are no real agglomerates in micron range revealed. This fact demonstrates that the compatibility of LDH with coating formulation is acceptable.

4.4 Shelf-life of the coating

4.4.1 EIS Results

The protection performance of the coatings developed in the lab and industrial conditions was studied using electrochemical impedance spectroscopy (EIS). This technique allows the assessment of the corrosion induced damage in the substrate and the coating barrier properties. The effect of storage time of the formulation on the corrosion protection performance of resulting coatings was evaluated by EIS.

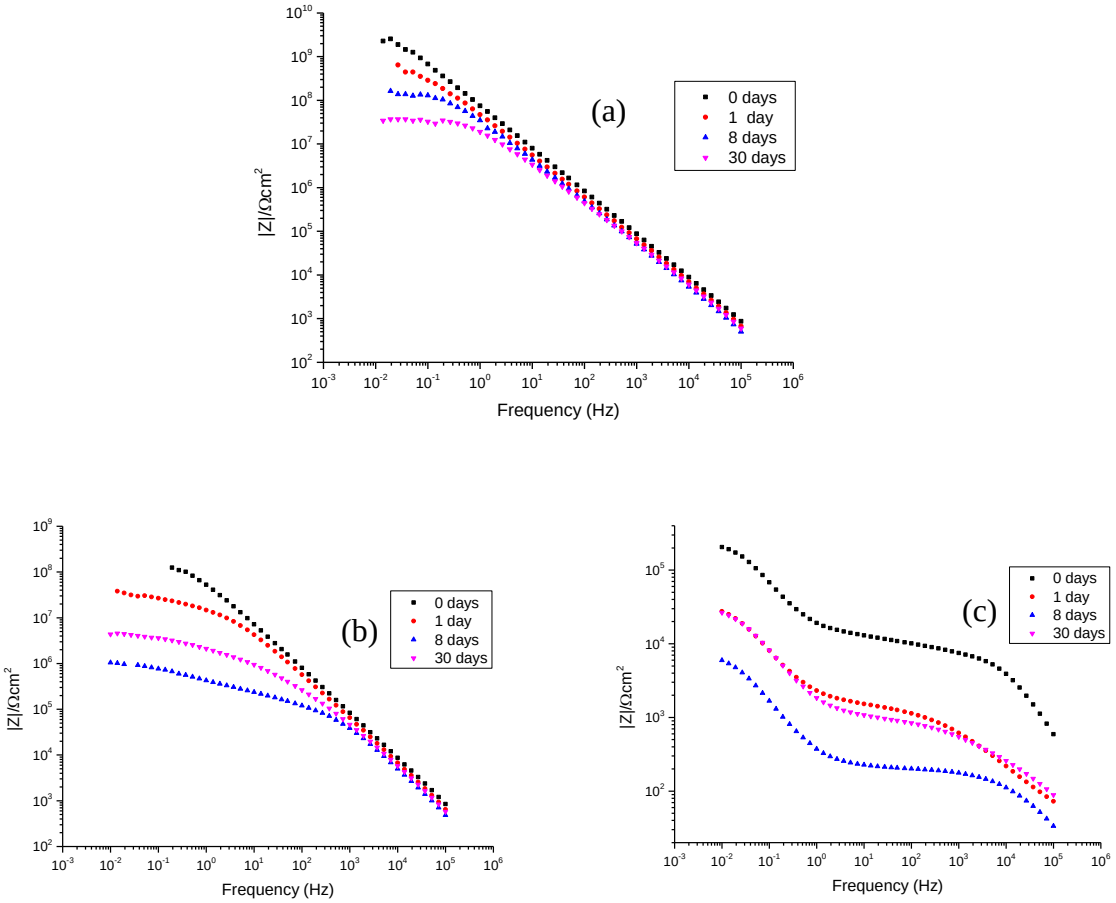

Figure 13 EIS spectra of 10%LDH-Gluc coatings prepared from formulations aged at different times. The results are presented for different immersion time in 0.5M NaCl: (a) 1 hour (b) 1 day (c) 28 days.

Figure 13 shows the EIS spectra of coatings prepared from formulations with different days of aging. The formulation used was 10%LDH-Gluc in the polymer. It is observed that after one hour of immersion in 0.5M NaCl one time constant for all coatings associated to capacitive responce from the coatings appeared. A decrease of impedance resistance is observed after 1 day of immersion, and a second time constant becomes well defined for formulations with 1, 8 and 30 days of aging. After the immersion time (28 days), a third constant time associated with corrosion processes appears and the impedance values are too low for formulations with 1, 8 and 30 days of aging. The value of impedance resistance for 10%LDH formulation with 0 days of aging is similar to the 10%LDH coating of Figure 20, roughly 10 $K\Omega cm^2$. The aging of formulation leads to a significant decrease of corrosion resistance which can be probably associated with the anionic exchange between species from the polymer formulation and gluconate.

4.4.2 XRD analysis

The shelf-life of the LDH-containing coating formulation as well as shelf-life of the LDH pigments is very important parameters when industrial applications of such systems are considered. In the present work XRD analysis was employed in order to understand if long-term storage has an effect on the crystalline structure of LDH and if any changes happen with intercalated anions. The LDH-slurry stored at open conditions for different periods of time were analysed.

According to literature there are different LDH polytypes [52], [53], the obtained XRD patterns of Zn-Al-Gluc (LDH-Gluc.) powder were not defined enough to distinguish among different LDH polytypes. So, for easy comparison of the crystal structure parameters, the XRD patterns studied of all compositions were indexed in the same “three-layer” 3R polytype.

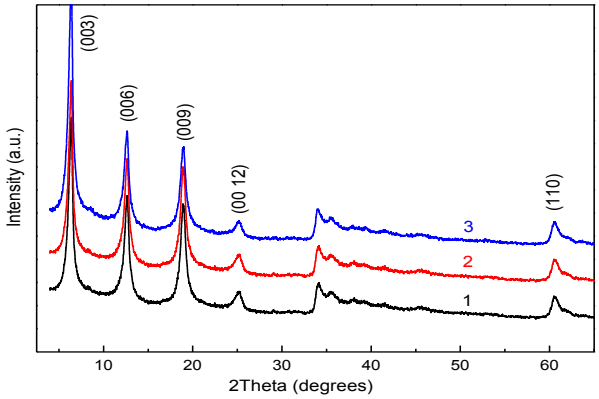

Figure 14 XRD patterns of Zn-Al-Gluconate LDH powders: as prepared (1), stored in slurry for 8 days and 1 month (2 and 3, respectively). The most representative diffraction reflections are presented

As it can be seen, there is no visible change in the patterns indicating that the storage in such conditions during 1 month has no effect on LDH-Gluc structure (Figure 14).

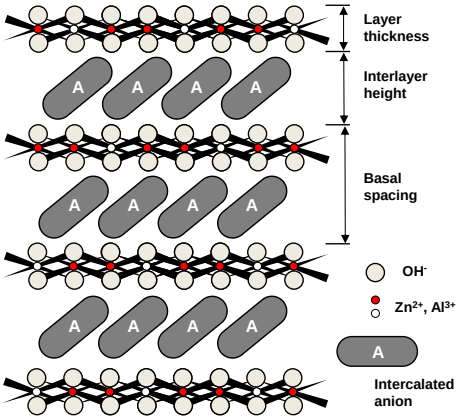

Figure 15 Schematic illustration of the layered structure of a Zn-Al LDH composition.

The patterns indicate a single-phase LDH structure with basal plane spacing value d~1.41 nm. Figure 15 schematically illustrates the basal plane spacing of LDH. The basal plane spacing is the distance between the adjacent hydroxide layers and is equal to $d_{(003)}$ in LDHs of 3R polytype.

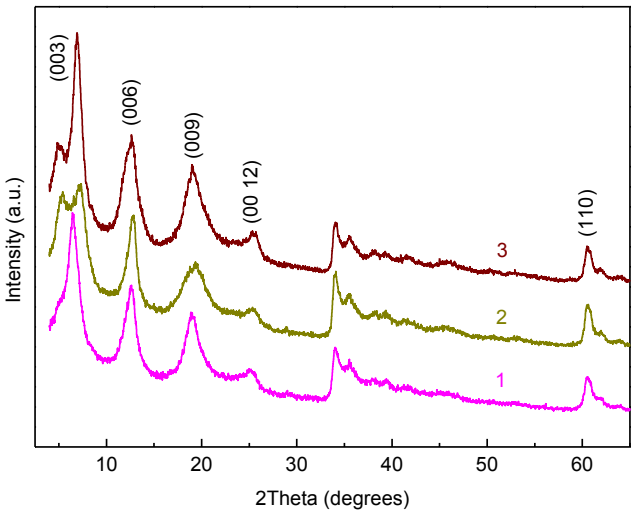

Figure 16 XRD patterns of Zn-Al-gluconate LDH powders immersed in the formulation for 1 day (1), 8 days (2), and 1 month (3).

The shelf-life of coating formulation was also studied with the immersion of LDH-Gluc powder in the polymer formulation. Figure 16 shows the XRD patterns of the samples immersed for different times. As the immersion time increases, the (003) reflections split into two peaks while other basal reflection broaden. These two peaks appeared on (003) reflection suggests appearance of layered structure with two different basal spacing values, at the same time, neither position nor shape of the (110) reflection changes indicating that the internal structure of the hydroxide layers remains unaffected.

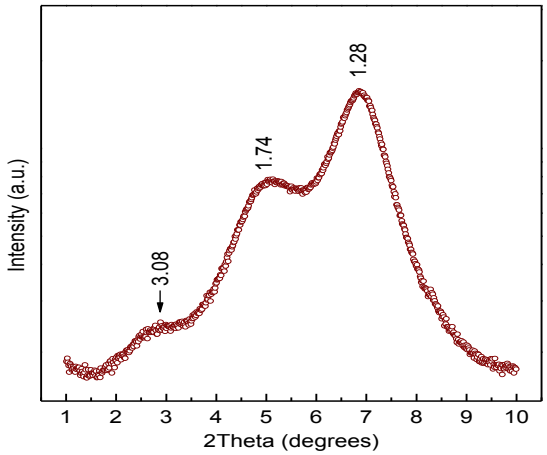

Figure 17 XRD pattern of Zn-Al-gluconate LDH powder immersed in the formulation for 1 month. Basal spacing values (in nanometers) corresponding to the low-angle XRD reflections are shown.

Low-angle XRD measurements of the sample immersed for 1 month revealed a diffraction peak at about 3° (Figure 17). Basal spacing value associated with this peak was found to be ~3.08 nm which can be represented as a sum of d_1≈1.28 nm and d_2≈1.74 nm (*d*-spacings of the peaks corresponding to the split reflection (003)).

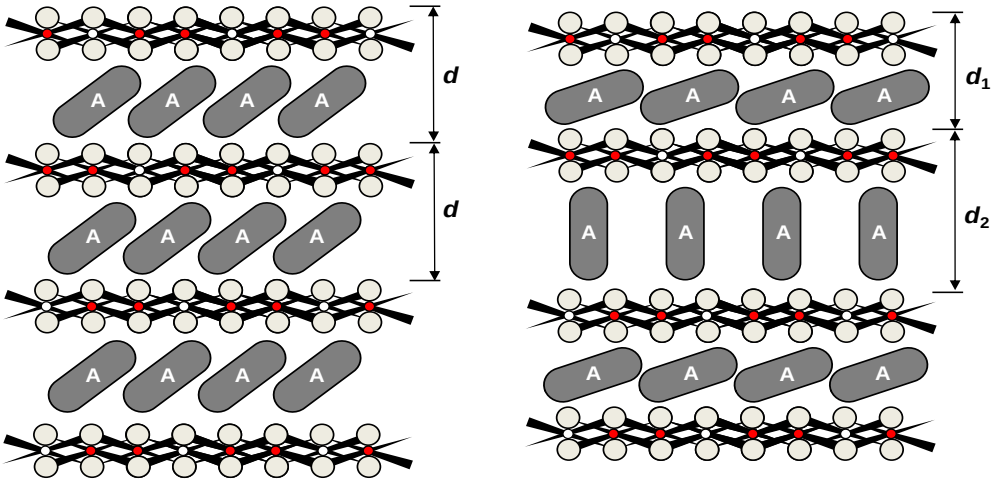

Figure 18 Possible rearrangement of the intercalated anions which results in appearance of alternating layers with basal spacings d_1 and d_2.

Figure 18 explains the effect of the values obtained in Figure 17, such effect is caused by alternating layers with different basal spacing. It results in appearance of the diffraction reflections corresponding to the values d_1, d_2 and d_1+d_2 [54]. Alternation of hydroxide layers with different *d*-spacing can be caused by both rearrangement of the intercalated anions and presence of two and more different anions in the inter layers. It is expected in this case that the intercalation of some species from the formulation which either substitute or supplement gluconate anions takes place.

Supplementary immersion experiments were undertaken (Figure 19-20) in order to reveal any interaction between LDH and the formulation. Zn-Al-carbonates and Zn-Al-nitrate were chosen as the test objects since CO_3^{2-} is hardly exchangeable while NO_3^- is easily substituted from LDH interlayers [55].

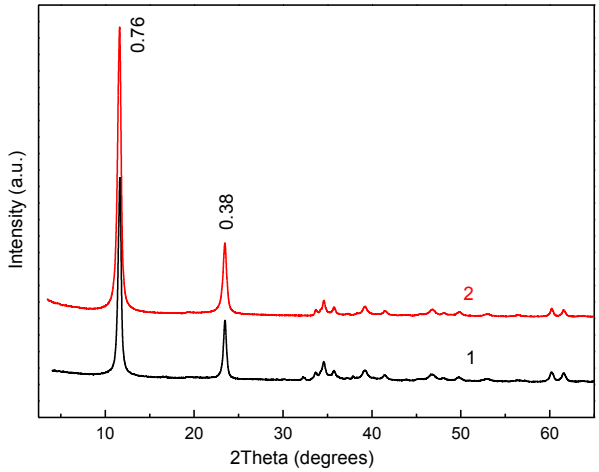

Figure 19 XRD patterns of Zn-Al-CO_3 LDH powder: as prepared (1) and immersed in the formulation for 10 days (2). Basal spacing values (in nanometers) corresponding to the (003) and (006) basal reflections are shown

As the same time, the XRD patterns of Zn-Al-NO_3 before and after 2 day immersion are fundamentally different (Figure 19) No trace of LDH-nitrate is observed in the immersed sample, while the peaks associated with the reflections (003) and (006) of an LDH-carbonate phase are present.

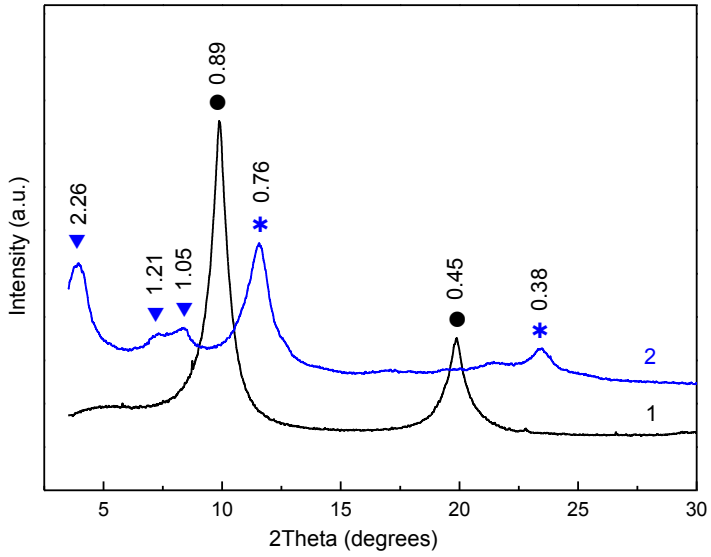

Figure 20 XRD patterns of Zn-Al-nitrate LDH powder: as prepared (1) and immersed in the formulation for 2 days (2).

Basal spacing values (in nanometers) corresponding to the basal reflections of Zn-Al-NO_3 (circles), Zn-Al-CO_3 (asterisks) and an LDH phase with alternating d_1/d_2 layers (triangles) are shown. Besides, the peaks which can be attributed to the basal reflections from the layers with the *d*-spacings $d_1' \approx 1.28$ nm, $d_2' \approx 1.74$ nm and $d' = d_1' + d_2'$ appeared in the XRD pattern (Figure 20), thereby indicating an LDH structure rather similar to that formed in the immersed Zn-Al-gluconate.

The Zn-Al hydroxide layer is 0.47 nm thick according to literature [56], the height of the narrowest interlayer in the immersed Zn-Al-nitrate is 0.81 nm (1.28-0.47). This value is considerably higher that the maximal dimension of the nitrate anion (0.51 x 0.48 x 0.24 nm) [57]. Despite of a multilayer of nitrate anions is possible; the most likely explanation is a gradual substitution/supplement of nitrate by some anion(s) from the formulation. A similar process seems to occur in the immersed Zn-Al-Gluconate as well.

The main conclusion from these measurements is that the LDH should be stored separately from the polymer formulation and mixed shortly before application if a long shelf-life of the formulation is expected.

4.5 Optimization of pigment concentration

It was studied the optimization of pigment in formulation, an optimum concentration allows better barrier properties of coatings on anticorrosion protection. Different concentrations were added from 1% to 20%wt of LDH in a dry film.

4.5.1 EIS results

In laboratory EIS measurements were carried out aiming at finding the optimal LDH concentration to be added to the coating formulation.

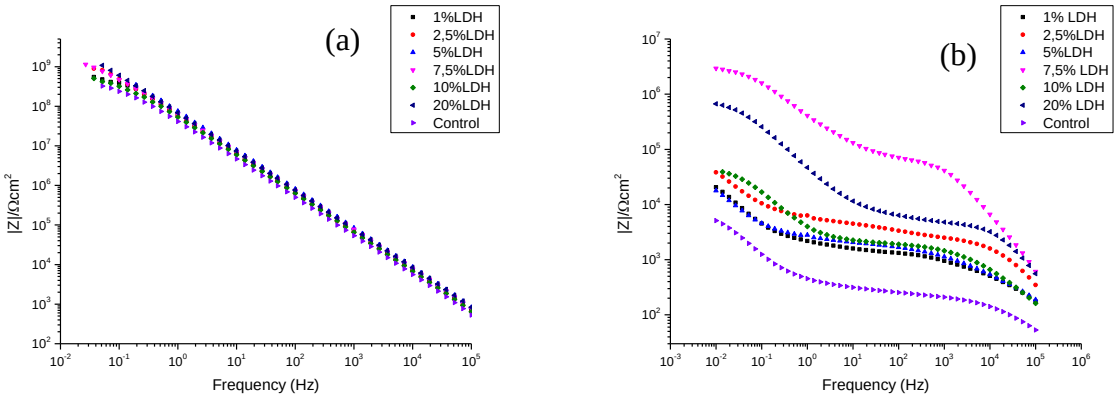

Figure 21 Impedance modulus spectra for the coatings with different concentration of LDH-Gluc after different immersion times in 0.5 MNaCl : (a) 1 day (b) 28 days

The optimal concentration of LDH pigment in the formulation was defined at laboratory on the basis of EIS analysis as well. Figure 21 shows that the initial impedance for all the samples is high (1G Ωcm^2 at 0.01 Hz).All the systems have a capacitive behaviour acting as an insulator. After 28 days of immersion two well-defined time constants are visible like in the case of industrial systems. The coating resistance is considerably different according to the amount of LDH added to the coatings. The highest value is achieved when 7.5% of LDH present in the coating. This concentration shows an optimal balance between the active protection and barrier properties. The system with 20% of LDH demonstrates lower barrier but the low frequency impedance still keeps high values confirming an efficient inhibition. Notice that blank system had the worst performance, with values significant below all the doped systems.

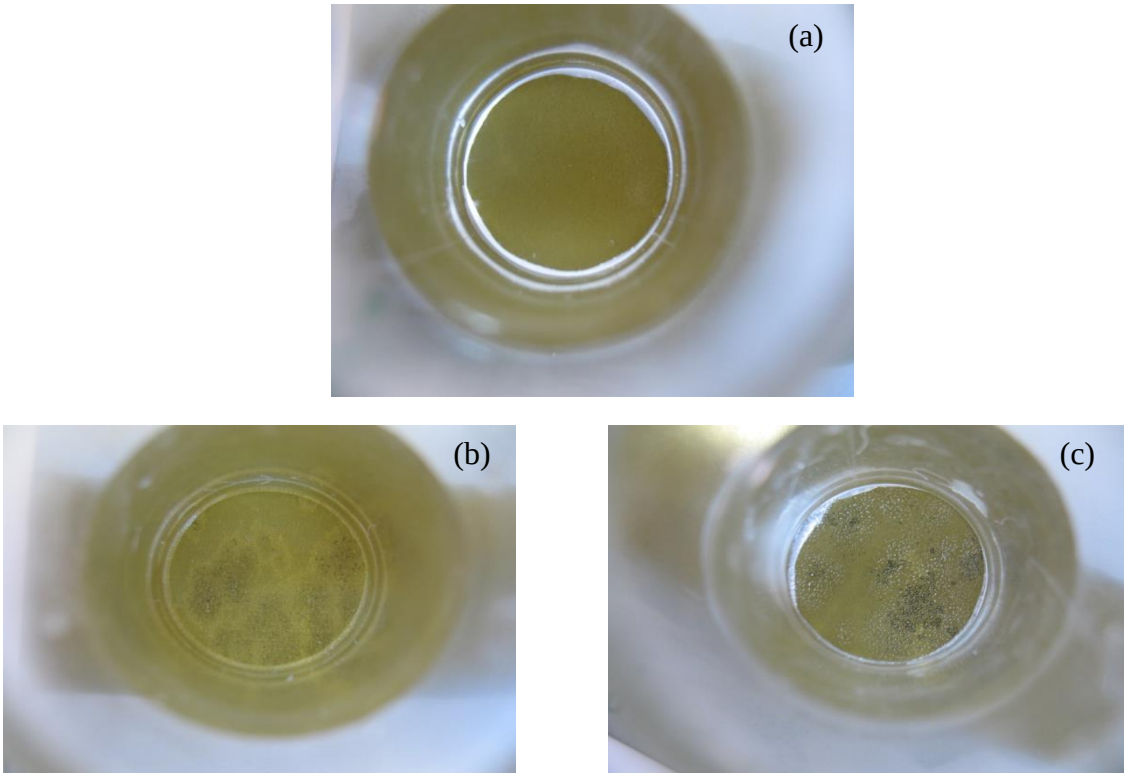

Figure 22 Photos of coatings after 28 days of immersion: (a) 7,5% LDH (b) 5% LDH (c) Control

Photos of coatings after 28 days of immersion in NaCl (Figure 22) were taken in order to understand how EIS results correlate with the coating appearance. Apparently no signs of corrosion are visible on 7,5%LDH coating comparing to control and 5%LDH. In control sample it is possible to observe that the surface is highly corroded through dark zones. In coating with 5%LDH, corrosion is clearly visible but not so high when compared to control may be due to a higher protection provided by LDH.

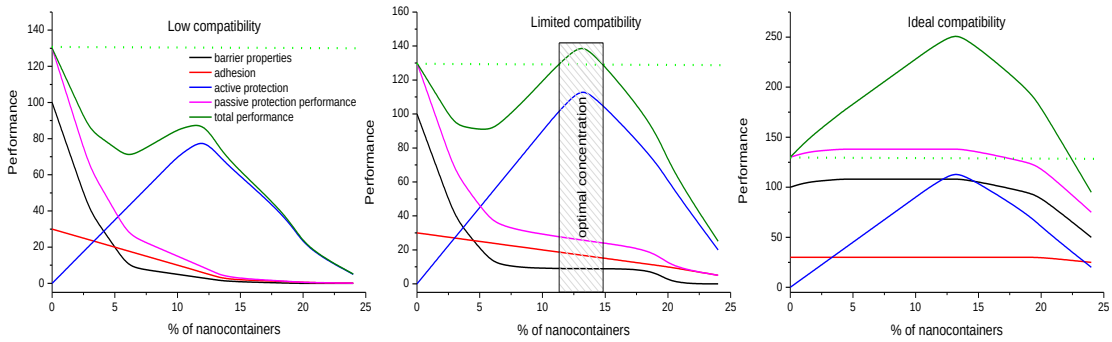

Figure 23 Protection coating system according to compatibility of nanacontaineres with polymer matrix

Figure 23 represents the effect of nanocontainer when added with the polymer matrix on performance of the protection coating system when they have low and limited compatibility for real situations. The total performance of a coating (green) depends on passive protection (pink) that includes adhesion (orange) and barrier properties (black). When nanocontainers are added to the formulation, extra protection is given to the coating with active inhibition (blue). The addition of nanocontainers in the coating will be a determining factor for the total performance of coating.

When nanocontainers have low compatibility with the coating formulation, very weak protection against corrosion is provided due to decrease of barrier properties. According to the graph in figure 23, the addition of small amount of nanocontainers leads to an abrupt decreasing of adhesion and barrier properties, resulting in the abruptly decrease of passive protection. When higher amounts of nanocontainers are added, it leads to a slight increase of total performance due to an increase of active protection. However, its performance is much lower when compared with a coating without nanocontainers. The addition of higher amount than 15%wt leads to the collapse of the coating due to agglomeration.

When nanocontainers have limited compatibility in the coating, the addition of small amounts leads to a continuous decrease of total performance and in middle concentrations the total performance remains constant but lower compared with smaller amounts. The addition of nanocontainers lead to a decrease of passive protection but the continuous addition of nanocontainers leads to a continuous increase of active protection until reaches an optimal concentration (11-14%) where the total performance is higher than a blank

coating. When studying LDH-Alg coating in ECC1, it is possible to make a comparison between its performance and graph of low compatibility of Figure 23. Figure 32 shows tthat the total performance of 2,5% is better than 5%wt but 10% shows the best results. Comparing control and 10%LDH-Alg, is possible to say that 10%LDH coatings have a similar or even slightly better performance than control.

Ideally, the addition of nanocontainers would not decrease the passive protection of the coating and an increasing amount of particles until the optimal concentration would lead to splendid coating performances (Figure 23).

4.6 Electrochemical tests of industrial coatings

EIS was also used to understand if the addition of LDH provides any positive effects on the coating performance for industrial samples.

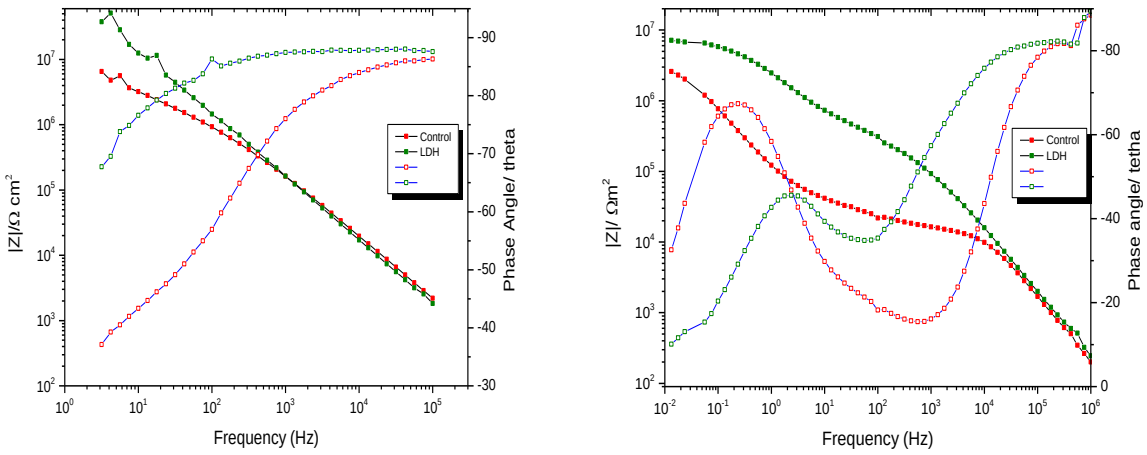

Figure 24 EIS bode for control and 5%LDH coatings obtained in industry after (a) 2 days and (b) 28 days after exposure to 5% NaCl

Figure 24 demonstrates the first results obtained on the industrial samples after different duration of immersion corrosion tests. After 2 days of immersion it was possible to observe one well-defined time constant for both coatings at high frequencies, this time constant can be attributed to a capacitive response from the coatings. The phase angle is between -90° and -80° at high frequencies revealing that coating behaves as capacitor. First signs of a second time constant appear on the control sample at middle frequencies. This relaxation process can be attributed to starting corrosion activities on the surface. So, after 2

days of immersion in 5% NaCl, LDH coating has a capacitive behavior and control starts loosing the protection properties. After 28 days of immersion the difference between the samples becomes even more obvious. The LDH-containing system keeps higher barrier and shows lower corrosion activities.

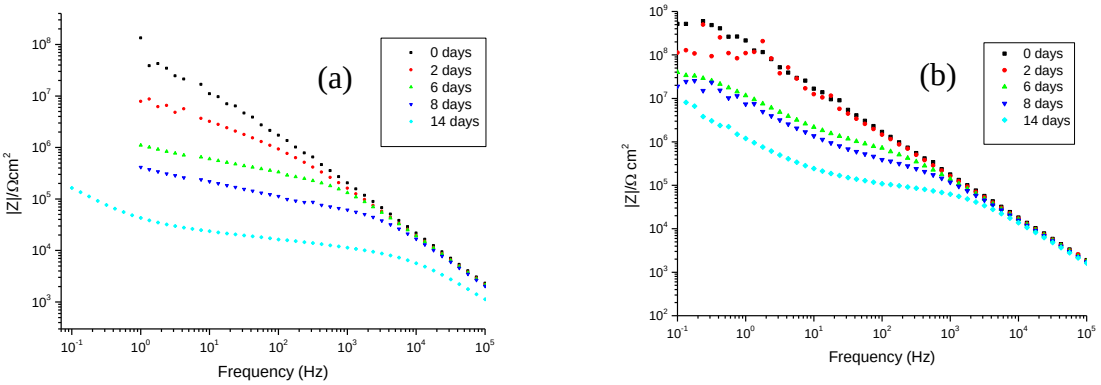

Figure 25 Evolution of impedance for different days of immersed 5% NaCl for: (a) control (b) LDH coatings

Figure 25 shows the evolution of impedance over time for control and coatings with LDH after immersion in a 5% NaCl. It is possible to observe that with the increase in immersion time the impedance starts to decrease. For shorter immersion times the impedance value for coatings with LDH was significantly higher than the control one. The impedance at low frequencies decreases almost one order magnitude after 2 days for blank coating. The second time constant associated to corrosion becomes visible. For coatings with LDH the impedance remains stable, presenting just one time constant, indicating that the system is capacitive and the coating maintains the barrier properties. After 6 days of immersion it is possible to observe that in coatings with LDH the second time constant starts to appear due to electrochemical activities. Its impedance value decreased almost one order magnitude. After 8 days, the impedance for both coatings decreased but it was more significant for the control system. After 14 days of immersion the further drop of performance is observed. But the LDH-containing system still keeps significantly higher impedance values. These results show a clear indication of the active protection provided by the addition of LDH particles loaded with gluconate. The fact that LDH are present in the

coating delays the appearance of new time constant and increases the anticorrosion performance of the coatings.

4.7 Accelerated corrosion tests

The corrosion protection performance was also studied using continuous (SST) and cyclic (ECC1) accelerated corrosion tests.

4.7.1 SST

Acidic salt spray is a type of accelerated corrosion test used in industry. A solution of 5% NaCl is continuously sprayed over the samples in a closed chamber with temperature 35°C and acidic medium (pH ~3). Coatings without particles (control), and LDH-Gluc, LDH-Alg were tested. Table 2 shows the concentration and specifications for each coating used.

Table 2 Samples specification for SST

Coating	LDH in coating (%)	Samples Tested	Observation
LDH-Alg	10	2	Dispersed with magnetic stirring
LDH-Alg	10	2	Dispersed with Turex
LDH-Alg	10	1	Dispersed with magnetic stirring coated on different day
LDH-Alg + LDH-Gluc	5	3	Dispersed with magnetic stirring
LDH-Alg + LDH-Gluc	2.5	3	Dispersed with magnetic stirring
Control	-	3	Dispersed with magnetic stirring

After 500 hours of SST, all samples presented red (oxide form of Fe) and white (hydroxide form of zinc) corrosion products formed on the scratches, due to the direct interactions between aggressive species from the surrounding medium and the GA layer of the scratch. Also in all samples, blisters appeared around the scratches and over the coating, resulting from corrosion.

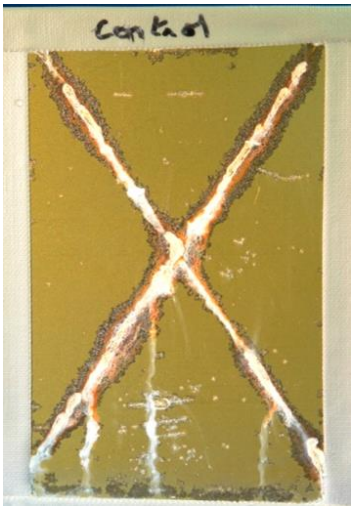

Figure 26 Control sample after 500 hours of SST

It was observed just for control samples, that around the blisters a darker coating colour appeared (Figure 26). This effect seems to be a result of coating delamination as a consequence of the lack of active protection provided by coating.

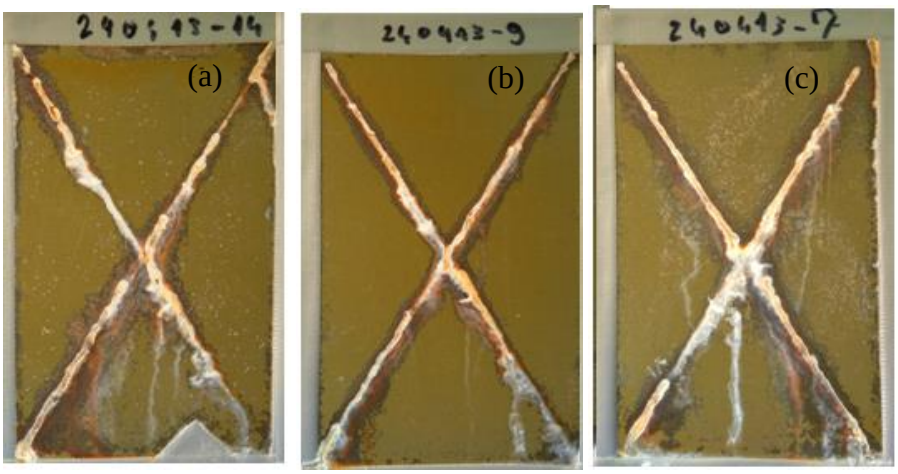

Figure 27 LDH-Gluc with different concentrations after SST: (a) 2,5% (b) 5% and (c)10%

Tiny white blisters appeared over LDH-Gluc creating roughness over sample surface (Figure 27). These type of blisters appeared just in this system, which can be a result of limited compatibility between LDH and coating that creates paths for aggressive corrosion species to reach the substrate and start reacting with the GA layer, forming white corrosion products. For all coating tested in SST, the sample that show better result was the 5%LDH-Gluc (Figure 27-b), the corrosion front over the scratch is not so large and there are few blister over the surface when compared with other samples. Reproducibility was very hard to achieve for the same conditions as can be compared in (Figure 27-a) and (Figure 27-b). Such effect could be a result of a deficient coating application that leads to the formation of defects.

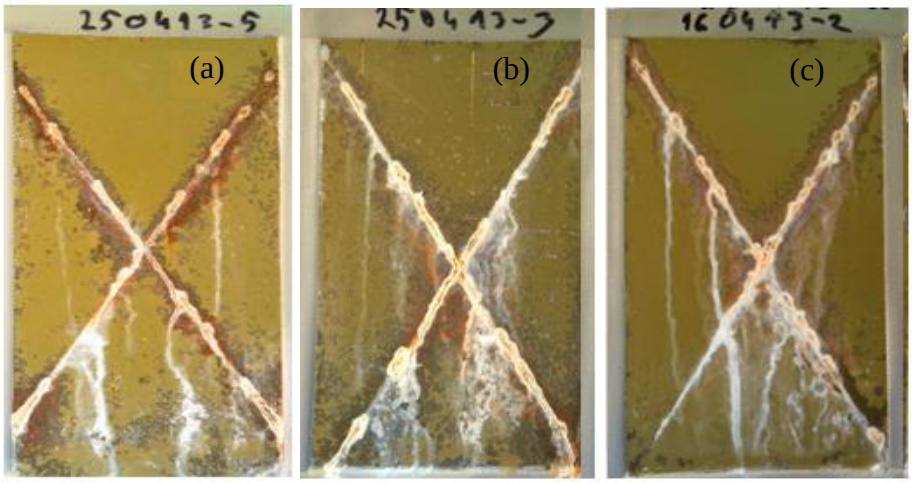

Figure 28 LDH-Alg with different concentrations after SST: (a) 2,5% (b) 5% (c) 10%

Figure 28 shows results of SST for the sample coated with formulation loaded with alginate-modified LDH. Comparing the samples observed in Figure 27, the LDH concentration performing better is 10%wt. of dry particles. Tiny white blisters of LDH-Gluc coatings did not appear in these coatings, this may be explained by a better compatibility of LDH in coating formulation due to the action of alginate. Comparing the three coatings tested, control was the one which had larger blisters. It was observed that the size of blister decreases with the increasing of LDH concentration.

The damage at scribe of samples was evaluated after SST. The maximal width at scribe caused by corrosion propagation and an average of delamination length in five different points at the scribe were measured (Figure 29). Also the surface quality of each

sample was evaluated and classified in very bad (1) to very good (10) (Figure 30). Surface quality is the number and roughness caused by blisters on coating surface.

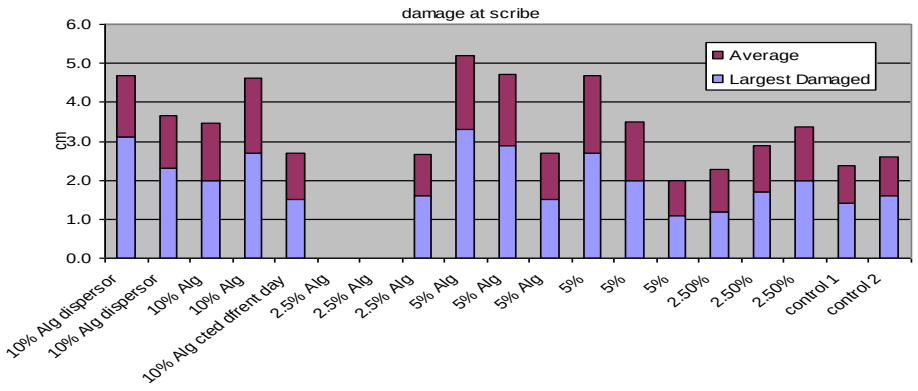

Figure 29 Damage at scribe for SST samples

Note that there is no classification for two samples of 2,5%LDH-Alg due to technical problems after the SST. According to Figure 28, control seems to have the best results, despite the existence of other samples that presented also good results (LDH-Gluc. 2,5% and LDH-Gluc 5%). The use of a dispersor (Turex), apparently shows no improvements when compared with magnetic stirring for 10% LDH-Alg as regards average damage at scribe. The systems that present the best results are control followed by LDH-Gluc.

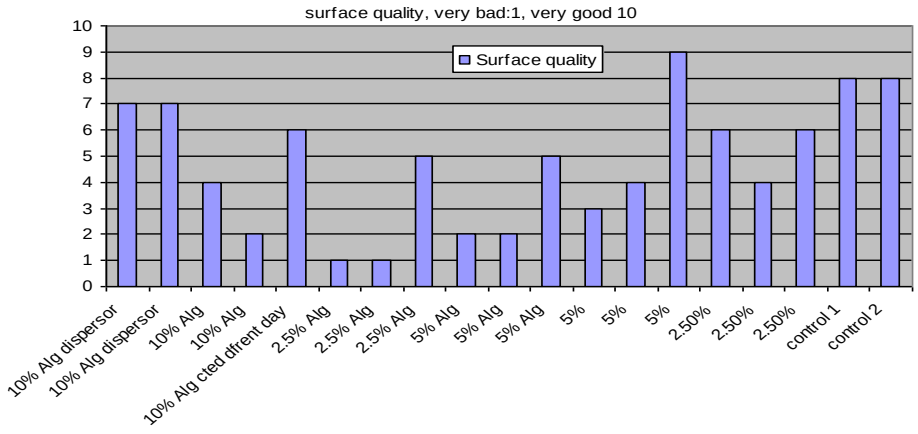

Figure 30 Classification for sample surface quality

Taking in to account the classification made in Figure 30, all the samples have defects over the surface, so the maximum classification (10) was not achieved. The best

sample grade was 9 and belongs to the 5%LDH-Gluc (Figure 27-b). Also both control and 10% LDH-Alg have good classification, 8 and 7 respectively. Comparing both types of particles, the LDH-Gluc seems to have better results. It was expected better performance for the majority of the coatings. However, because this classification was done based on visual analysis, the existence of errors should not be neglected.

4.7.2 ECC1

ECC1 (Cyclic corrosion tests) is a type of cyclic accelerated corrosion test used in the industry. During the experiment the relative humidity (%) and temperature (°C) were changed as indicated. ECC1 ran for 10 weeks, with a check after 3 weeks. The performance of coatings with different LDH-Alg concentration and a control one was compared.

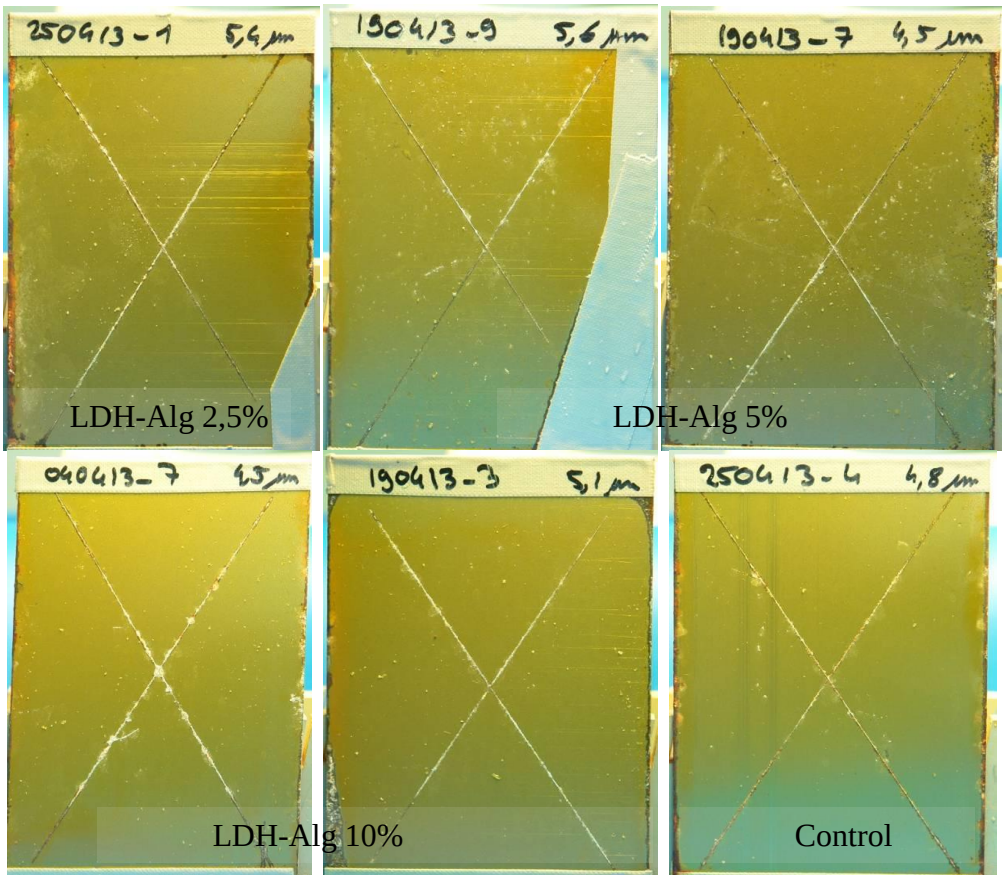

Figure 31 Samples after 3 weeks of ECC1 test

After three weeks of ECC1 test (Figure 31), no significant conclusions can be drawn by observing the samples. It was noticed that corrosion products and defects start appearing along the scribe and over the sample surface. The samples which present the worst results were the 5% LDH coating.

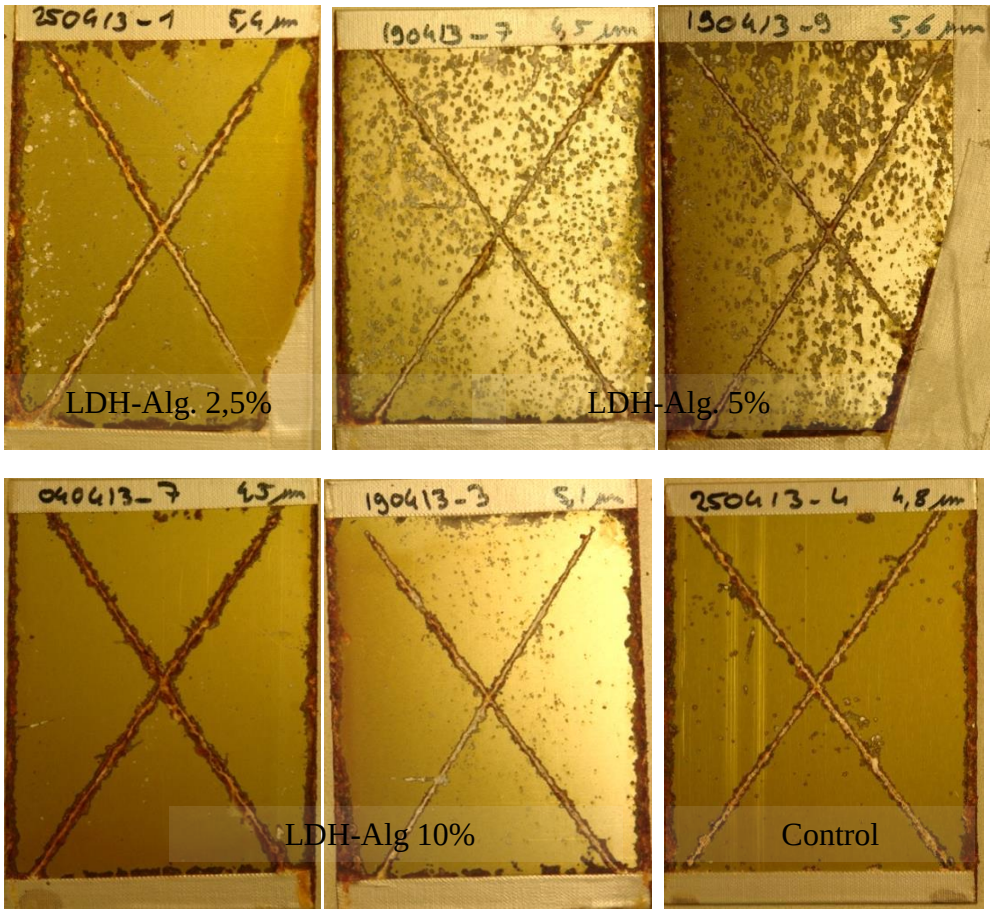

Figure 32 Samples after10 weeks of ECC1 test

Figure 32 represents the samples after 10 weeks of ECC1 test. LDH system presents better results comparing the damage formed over the surface for control and 10% LDH-Gluc. For control samples, there are big defects and bare metal is observed. For LDH just tiny defects appears on the surface. It may indicate that in control there is nothing that hampers corrosion propagation, which leads to delamination. Comparing sample (a) and (b) of 10% LDH-Alg it is possible to verify that sample (a) has very few defects on surface, nonetheless in sample (b) some defects are observed. Such observation may be explained by the difference in coating thickness, with higher thickness, as observed in sample (b), the coating is more susceptible to defects formation.

It is possible to speculate with ECC1 tests that LDH-Gluc alg. 10% coatings have better corrosion protection when compared to the control one. In the case of control the propagation of defects on the original surface is more obvious. However damage at the scribe is similar or even lower when compared to the LDH-containing coating. Coating 10%LDH-Alg seems to be a good option in the future for industrial application because no coating delamination and propagation on defects is observed.

4.8 Micro-analyses of corrosion processes

Optical microscope images of three different coatings (control, LDH-Gluc and LDH-Alg) were obtained to observe the appearance of blisters over the surface after SST. The effect of corrosion in the coating and substrate was studied by SEM with aim to understand how corrosion defects appear and develops in the coating.

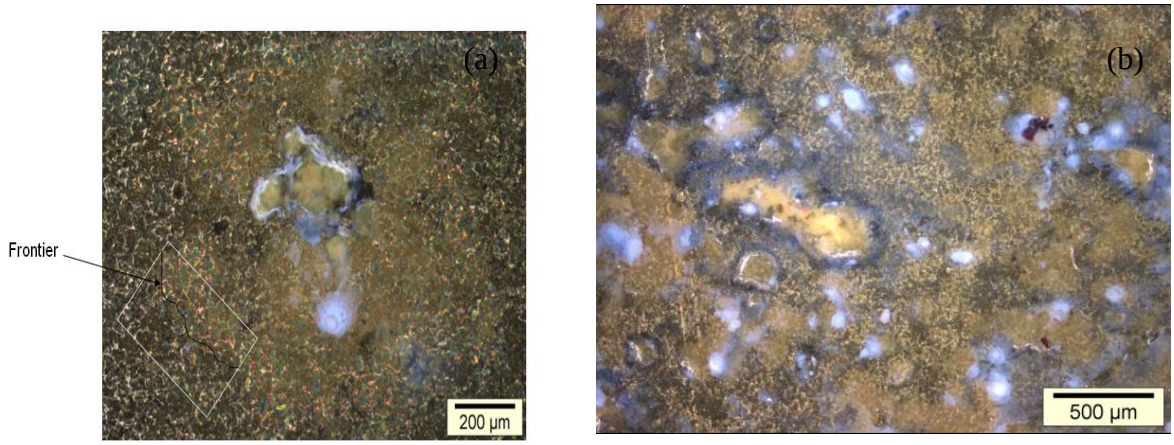

Figure 33 Appearance of blister over the surface: (a) control (b) LDH-Gluc with magnification x10 and x 5 respectively

It was mentioned that after SST, a visible colour contrast appeared just on the surface of control sample indicating possible delamination and roughness with tiny white defects appeared on LDH-Gluc coatings. It is possible observe on Figure 33-a, a colour contrast on the coating, there is a big area of damaged coating around the blister until it reaches a frontier (Figure 33-a) where the coating affected. The image (b) shows a corroded area on the surface of LDH-Gluc sample. Two types of defects are observed: one with a black line surrounding the defect and the other with white defects which are spread on the coating as it is shown on the image.

There is a large damaged area around the blister on the control sample, such defect come from the corrosion front under the coating that contribute for coating delamination. The explanation for such a large corrosion front may be the lack of active corrosion protection. In the case of LDH-containing system the morphology of defects is significantly different. The large blisters are normally not observed. Instead many small defects with white corrosion products on top are identified. The appearance of tiny white defects on LDH-Gluc surface may be a result of limited incompatibility between LDH and polymer that creates pathways between coating and surrounding medium. These paths should allow the direct access of oxygen and corrosive species which reacts with the zinc from GA surface. Zinc creates zinc hydroxides, corrosion products that progress through the coating reaching the surface.

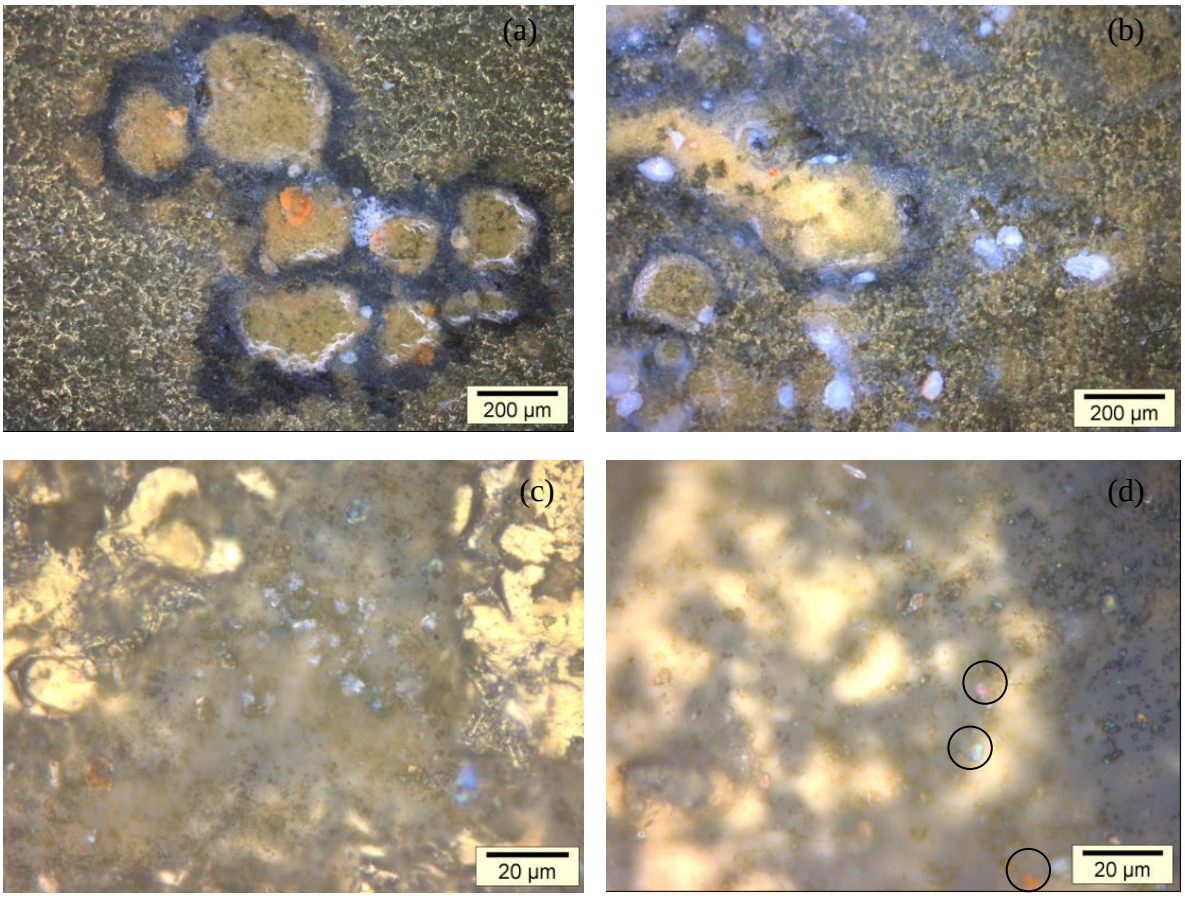

Figure 34 Images of LDH-Alg: (a) magnification x 10 and (c) maginification x 50; image for LDH-Gluc: (b) magnification x 10 (d) magnifications x 50

Image (a) and (b) of figure 34 shows the blisters formed on LDH-Alg and LDH-Gluc coatings respectively. It is observed that blisters appear on the coating as agglomerates with a black contour. While in LDH-Gluc the blisters appear more spread over the coating.

Higher magnification (x 50) was applied in areas where no signs of corrosion were visible with aim to observe how corrosion develops in the relatively intact areas as observed in image (c) and (d) of Figure 34. The defects on LDH-Alg appear as blue points, these are concentrated in a certain area of the coating. The defects on LDH-Gluc are spread over the coating surface as orange, blue and pink points represented as circles on (Figure 34-d). They appear on the coating, possibly due to the micro-bubbles observed on coating application (Figure 10-b). The colour contrast observed can be due to deposition and diffusion of aggressive species in the micro-bubbles. These points could be initial zones for blister formation and growth.

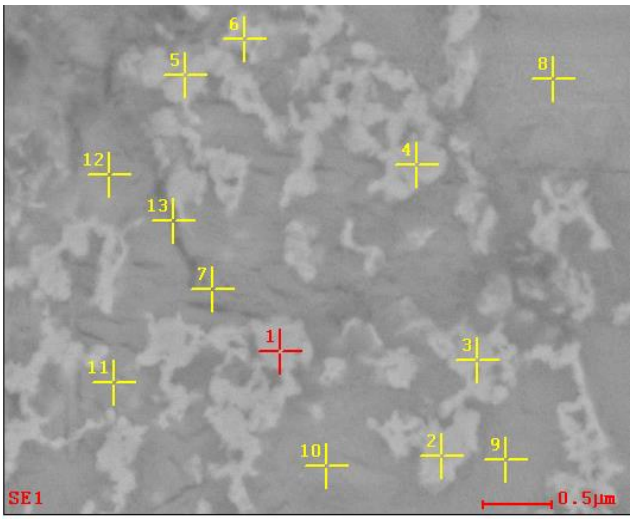

Figure 35 Micrographic of GA layer

GA layer is a Fe-Zn alloy and is composed by different Fe-Zn phases. Figure 35 presents the macrograph of GA layer in areas where corrosion starts. The image has different colours derived from different Fe and Zn content.

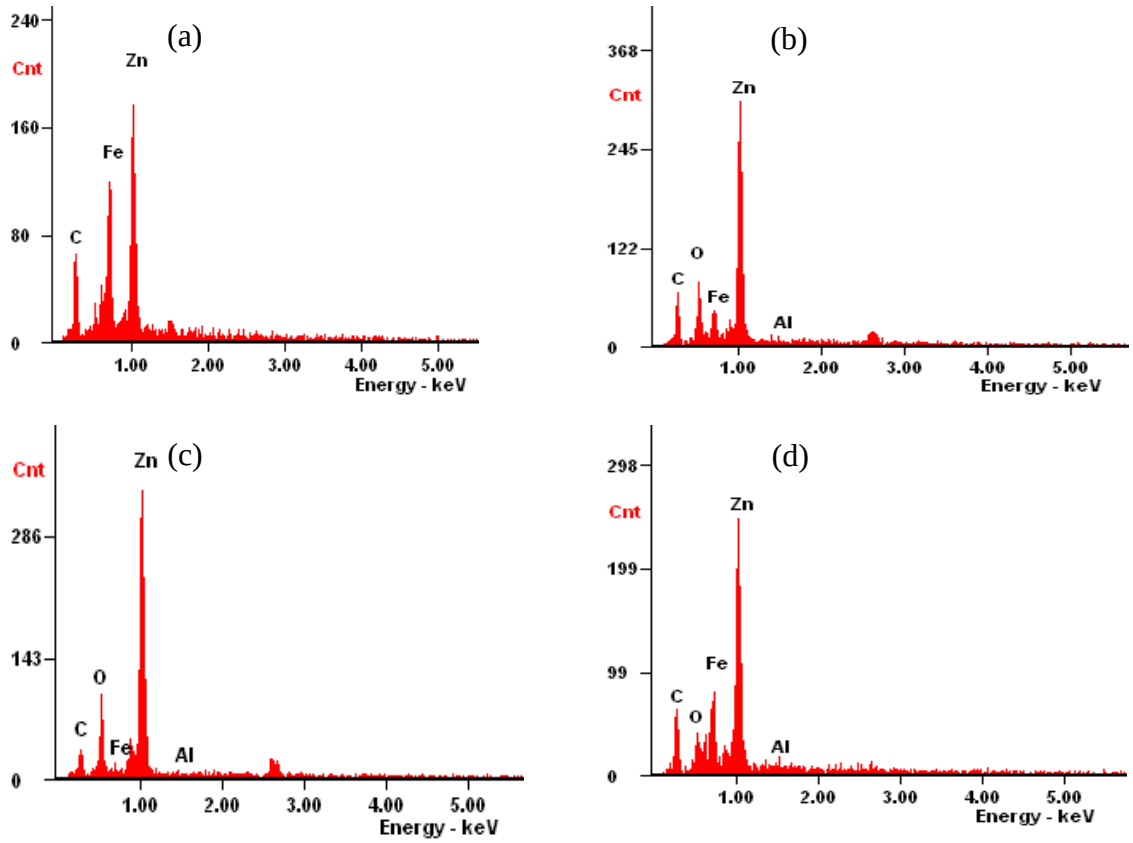

Figure 36 EDS of figure 35 for different points: (a) 1 (b) 11 (c) 8 (d) 6

Figure 36 shows EDS spectrums for different points of Figure 35. The phase represented as point 1 of Figure 35 is bright and no sign of corrosion is observed. Its EDS (Figure 36-a) reveals that is composed mainly by Zn and Fe. The point 6 is not as bright as the 1. It is observed that in its EDS (Figure 36-d) the content of Fe decreases and O increases which can be associated to oxidation of Fe. Finally the phase of point 8 is the one more corroded. The content of Fe (Figure 36-c) is almost zero. The content of oxygen is higher of all of them and the content of Zn decreases when compared with point 11 which could be associated with Zn oxidation.

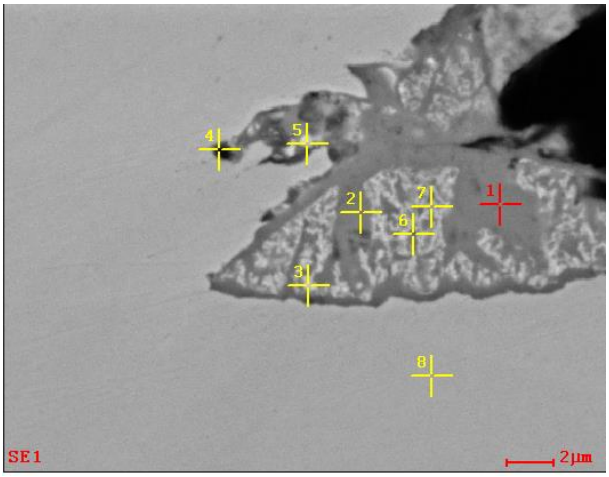

Figure 37 SEM micrograph of control sample beside the scribe after corrosion

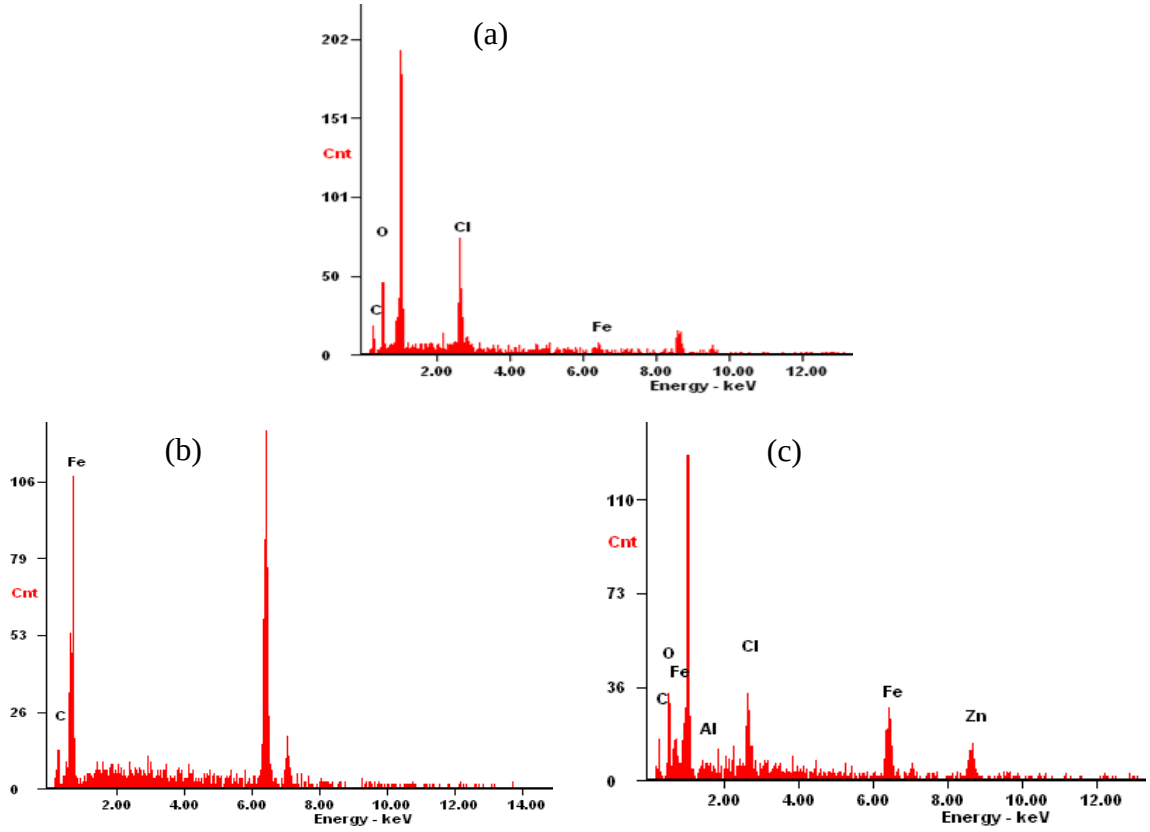

Figure 38 EDS of figure 37 for different points: (a) 1 (b) 8 (c) 6

The micrograph of Figure 37 was taken close to the scribe. It is observed the coating (black), the substrate (grey) and the GA layer (with dark and bright areas) with different phases. The EDS for the substrate (point 8) is observed on Figure 38-b. The substrate has high content of Fe. The EDS spectrums (a) and (c) of Figure 38 belongs to two

different phases on GA layer (point 1 and 6 respectively). Comparing both spectrums, the content of Fe and Zn is roughly 6,3 and 8.3 keV shows that corrosion in point 1 is more significant than in point 6. Also, the content of Cl is higher in the spectrum more corroded. Corrosion processes on GA layer are associated to a decreasing of Fe content due to its oxidation. With these spectrums is possible to conclude that corrosion appears in areas with lower content of Fe.

Corrosion appears on different stages for different GA phases. Phases with lower content of Fe (point 1) will sacrificially protect phases with higher Fe (point 6) content because Fe is nobler when compared to Zn.

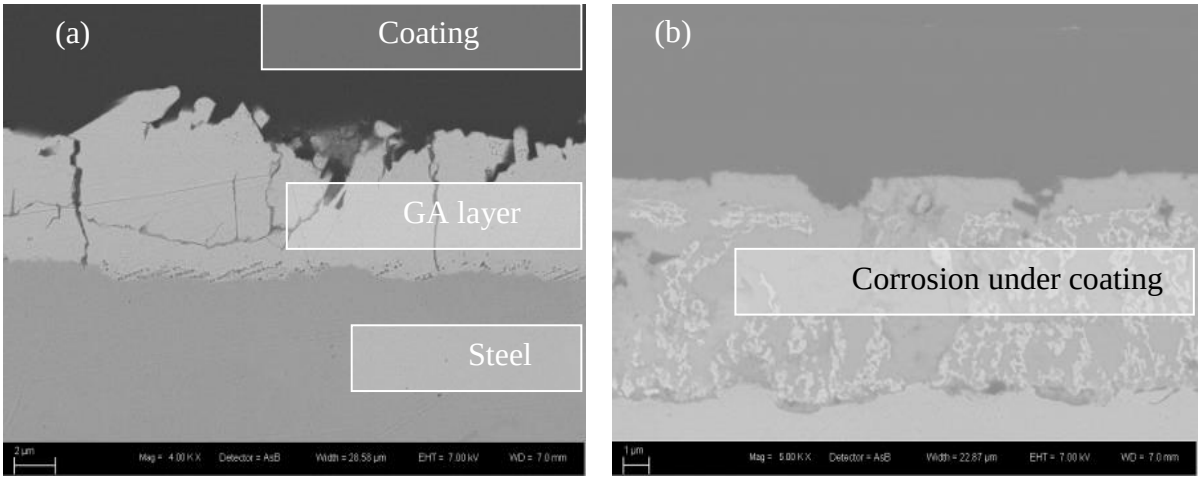

Figure 39 Components of a coating (a) and corrosion on GA layer (b)

Image (a) in figure 39 presents the cross section of the coated substrate. Different layers can be seen on the image. Steel is sacrificially protected against corrosion by a GA layer with the coating providing an extra barrier protection. No sign of corrosion is observed before corrosion tests on image (a). Image (b) indicates that during the accelerated weathering tests corrosion starts under the coating with the damaging of GA layer as can be seen from the presence of bright and darker zones verified by EDS spectrums from the magnification of Figure 37.

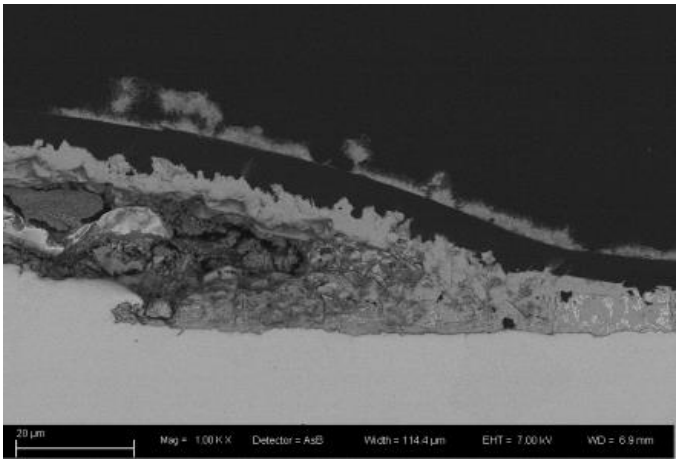

Figure 40 Micrograph of a blister side

A blister is a result of an increase in volume of corrosion products on the GA layer that leads to coating delamination. Figure 40 shows a cross-section of a blister. Blister appeared from the reaction of zinc with the aggressive species. Aggressive species reach GA layer through diffusion or penetration into some cracks present on the coating. Corrosion products can reach the coating surface through diffusion forming fine layers of corrosion products above the polymer film.

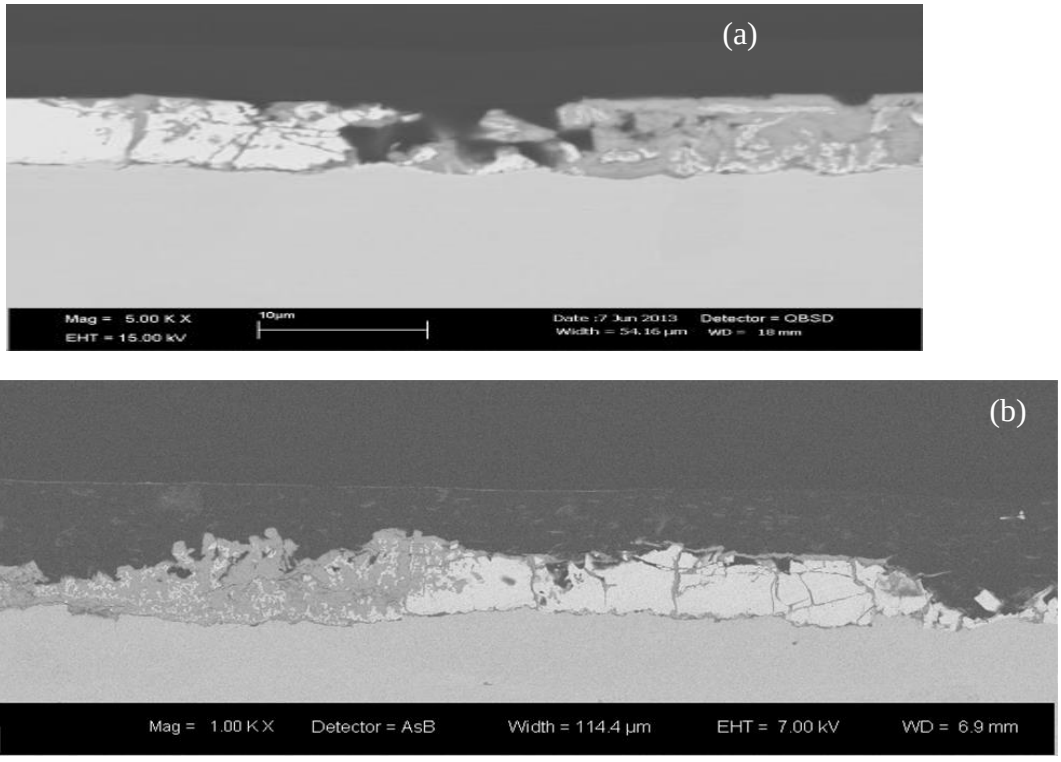

Figure 41 Corrosion front for: (a) control and (b) coating with LDH

Figure 41 demonstrate the corrosion front propagation for control sample (image a) and the one coated with LDH-containing polymer (image b).The propagation of the corrosion front is different in the case of these two systems. The corrosion front for control sample is developing with strong dissolution of the sacrificial GA layer. The GA layer in the case of inhibited system is destroyed at lower extent probably because of active protective action of inhibitor.

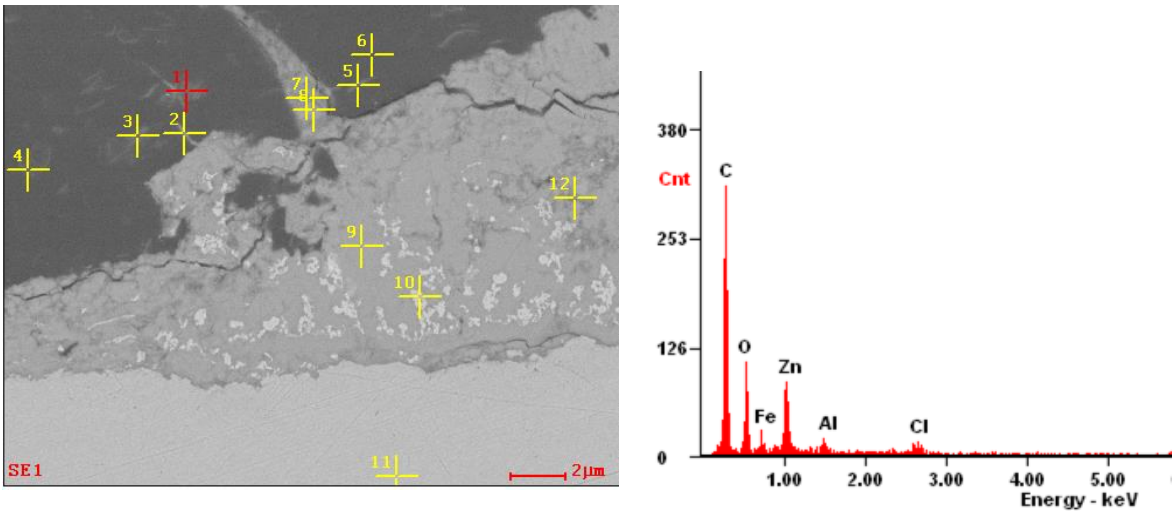

Figure 42 EDS spectrum for point 1 of image

The image of figure 42 shows the edge of a blister where it is possible to observe the substrate, the GA layer with different corrosion products. The EDS spectrum taken in the place of larger LDH particle can contribute to the understanding of the active corrosion protection provided by the inhibited system. A well defined signal of Cl can be detected. Original LDH is loaded with gluconate anion and does not have any chlorides. The chloride can appear at high concentration in the location of the LDH particle only as a result of anion exchange process. As it is reported before [42] the chlorides can substitute anions in the LDH leading to triggered release of the inhibiting ion. Thus, when anionic specie (Cl^-) is diffusing through the coating and when in presence of LDH, they release the corrosion inhibitor and at the same time entrap anionic species decreasing and hampering corrosion activity.

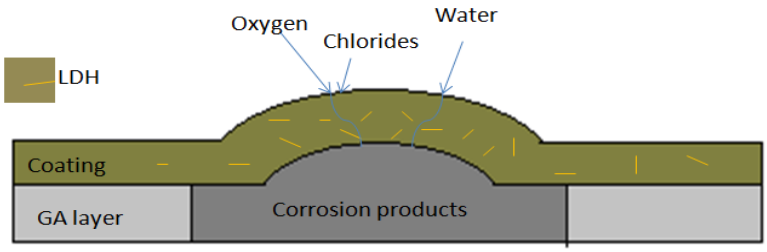

Figure 43 Formation of a blister for LDH coatings

The size of blisters varies according to the coating tested. The blank sample shows the bigger blisters. Figure 43 schematically illustrate the formation of blisters. For control samples, aggressive species (oxygen, chlorides and water) cross the coating through diffusion and defects. When LDH-Gluc is added to the coating, it provides an additional active effect. The observed volume of corrosion products was not so high when compared to the control system and corrosion front does not propagate as fast as a result of inhibition. In the case of LDH-Alg an additional barrier for diffusion of aggressive species is created because of the ordered parallel structure which increases a diffusion path. .

When the LDH concentration is increased, both coatings showed a decrease in the blisters size due to high amount of LDH, that provides an active protection as well as additional barrier. The combined effect of the barrier and the active protection hampers the formation of corrosion products and reduce propagation of the corrosion front.

CHAPTER 5

Conclusions and Future Work

5. Conclusions and Future Work

The present work allowed understanding of important parameters concerning up-scaling challenges for LDH-containing active protection coatings. DLS measurements indicate reasonable compatibility between LDH and coating formulation. Such compatibility show that is acceptable the use of LDH pigments with this coating formulation for active protection coatings. The shelf-life of LDH in storage conditions and in polymer formulation was studied using XRD analyses and EIS measurements. The EIS measurements demonstrate that LDH remained in coating formulation during aging time weakens coating barrier properties. XRD analyses showed no changes in LDH crystalline structure when aged in storage conditions. On the other hand, it was demonstrated that crystalline structure of LDH in coating formulation changed with aging time. This difference is associated to anion-exchange between gluconate and anions from formulation. The main conclusion from these measurements is that the LDH should be stored separately from the polymer formulation and mixed shortly before application if a long shelf-life of the formulation is expected.

The surface modification of LDH with alginate allows a faster and effective dispersion in the coating formulation as well a good order in the coating. It is possible to achieve higher active protection from LDH when they are well ordered in the coating matrix. The optimization of LDH in coating matrix was studied by EIS measurements. The results showed not only that the best concentration tested was 7,5%LDH but also showed that the addition of LDH allows higher impedance values and a delay on the appearance of new time constants.

Corrosion of the samples was verified after tested in accelerated corrosion tests. The results showed that different corrosion mechanisms appear according to the coating system used which are associated to no active protection for control samples and different compatibilities between LDH with and without alginate.

For further work it is suggested studying with more detail which anions from polymer formulation are intercalating in LDH-galleries. Also a study in order to increase compatibility between LDH and polymer formulation is needed.

References

References

1. Talbot, D.E.J. and J.D.R. Talbot, *Corrosion Science and Technology*2010: Taylor & Francis.

2. Schutze, M., *Corrosion and Environmental degradation*. 1 edition ed, ed. P.H. R.W.Cahn, E.J.Krammer. Vol. Vol. II. April 7, 200: Wiley-VCH.

3. McCafferty, E., *Introduction to Corrosion Science*2010: Springer.

4. Roberge, P., *Handbook of Corrosion Engineering*1999: Mcgraw-hill.

5. Money, K.L., *Corrosion Testing in the Atmosphere*, ed. M.H. Corrosion1987, Meatls Park, Ohio: ASM Internationl.

6. Shreir, L., *Corrosion, Vol 2: Corrosion Control, Edited by L.L. Sheir and Others*1994: Butterworth.

7. Ahmad, Z., *Principles of Corrosion Engineering and Corrosion Control*2006: Elsevier Science.

8. Davis, J.R., *Corrosion: Understanding the Basics*2000: A S M International.

9. Scully, J.C., *The fundamentals of corrosion*1990: Pergamon Press.

10. Ralph W.Leonard, C.S.T., LLC, *Continuous Hot Dip Coatings*. Corrosion: Fundamentals, Testing, and Protection. Vol. 13A. 2003.

11. Association, A.G., *Zinc Coatings.*

12. *Hot Dip Galvanizing for Corrosion Protection of Steel Products*. 12.

13. Zin, I.M., *Corrosion inhibition of galvanized steel with inorganic pigments.* Materials Science, 1999. **35**(6): p. 874-878.

14. LCB, B., *Literature Review for Red Rust problem*2002.

15. Jones, L.W., *Corrosion and water technology for petroleum producers*1988: OGCI Publications.

16. Philip A. Schweitzer, P.E., *Fundamentals of Corrosion: Mechanisms, Causes, and Preventative Methods*2009: Taylor & Francis.

17. Zhang, X.G., *Corrosion of Zinc and Zinc Alloys*, in *Corrosion: Materials*, A. Handbook, Editor 2005, ASM International. p. 402 - 417.

18. Munger, C.G. and L.D. Vincent, *Corrosion Prevention by Protective Coatings*1999: National Association of Corrosion Engineers.

19. Tedim, J., et al., *Enhancement of active corrosion protection via combination of inhibitor-loaded nanocontainers.* ACS Applied Materials and Interfaces, 2010. **2**(5): p. 1528-1535.

20. Ferreira MGS, Z.M., Tedim J and Yasakau KA, *Self-healing nanocoatings for corrosion control*, in *Corrosion protection and control using nanomaterials*2012, Woodhead Publishing Limited.

21. Kumar, A., L.D. Stephenson, and J.N. Murray, *Self-healing coatings for steel.* Progress in Organic Coatings, 2006. **55**(3): p. 244-253.

22. Sugama, T. and K. Gawlik, *Self-repairing poly(phenylenesulfide) coatings in hydrothermal environments at 200 °C.* Materials Letters, 2003. **57**(26–27): p. 4282-4290.

23. Zheludkevich, M., *Self-Healing Anticorrosion Coatings*, in *Self-Healing Materials*2009, Wiley-VCH Verlag GmbH & Co. KGaA. p. 101-139.

24. Zarras, P., et al., *Progress in using conductive polymers as corrosion-inhibiting coatings.* Radiation Physics and Chemistry, 2003. **68**(3–4): p. 387-394.

25. Zheludkevich, M.L., et al., *Anticorrosion Coatings with Self-Healing Effect Based on Nanocontainers Impregnated with Corrosion Inhibitor.* Chemistry of Materials, 2007. **19**(3): p. 402-411.

26. Lamaka, S.V., et al., *TiOx self-assembled networks prepared by templating approach as nanostructured reservoirs for self-healing anticorrosion pre-treatments.* Electrochemistry Communications, 2006. **8**(3): p. 421-428.

27. Conde, A., A. Durán, and J.J. de Damborenea, *Polymeric sol–gel coatings as protective layers of aluminium alloys.* Progress in Organic Coatings, 2003. **46**(4): p. 288-296.

28. Zheludkevich, M.L., et al., *Corrosion protective properties of nanostructured sol–gel hybrid coatings to AA2024-T3.* Surface and Coatings Technology, 2006. **200**(9): p. 3084-3094.

29. Zhang, X.-l., S.-l. Zhang, and Y. Lei, *Corrosion Resistance of in-Situ Phosphatizing Organic Coating Modified with Rare Earth Oxide Nanoparticles.* Metal Finishing, 2012. **110**(7): p. 24-28.

30. Shchukin, D.G., et al., *Layer-by-layer assembled nanocontainers for self-healing corrosion protection.* Advanced Materials, 2006. **18**(13): p. 1672-1678.

31. Falcón, J.M., F.F. Batista, and I.V. Aoki, *Encapsulation of dodecylamine corrosion inhibitor on silica nanoparticles.* Electrochimica Acta, (0).

32. Shchukin, D.G., et al., *Active anticorrosion coatings with halloysite nanocontainers.* Journal of Physical Chemistry C, 2008. **112**(4): p. 958-964.

33. Zheludkevich, M.L., J. Tedim, and M.G.S. Ferreira, *"Smart" coatings for active corrosion protection based on multi-functional micro and nanocontainers.* Electrochimica Acta, 2012. **82**(0): p. 314-323.

34. Borrelli, R.A., O. Thivent, and J. Ahn, *Parametric studies on confinement of radionuclides in the excavated damaged zone due to bentonite type and temperature change.* Physics and Chemistry of the Earth, Parts A/B/C, 2013. **65**(0): p. 32-41.

35. P. Newman, S. and W. Jones, *Synthesis, characterization and applications of layered double hydroxides containing organic guests.* New Journal of Chemistry, 1998. **22**(2): p. 105-115.

36. Duan, X. and D.G. Evans, *Layered Double Hydroxides*2006: Springer.

37. Zheludkevich, M.L., et al., *Active protection coatings with layered double hydroxide nanocontainers of corrosion inhibitor.* Corrosion Science, 2010. **52**(2): p. 602-611.

38. Bohm, S., et al., *Novel environment friendly corrosion inhibitor pigments based on naturally occurring clay minerals.* Werkstoffe und Korrosion, 2001. **52**(12): p. 896-903.

39. Buchheit, R.G., et al., *Active corrosion protection and corrosion sensing in chromate-free organic coatings.* Progress in Organic Coatings, 2003. **47**(3–4): p. 174-182.

40. Kovanda, F., et al., *Preparation of layered double hydroxides intercalated with organic anions and their application in LDH/poly(butyl methacrylate) nanocomposites.* Applied Clay Science, 2010. **48**(1–2): p. 260-270.

41. Montemor, M.F., et al., *Evaluation of self-healing ability in protective coatings modified with combinations of layered double hydroxides and cerium molibdate nanocontainers filled with corrosion inhibitors.* Electrochimica Acta, 2012. **60**(0): p. 31-40.

42. Tedim, J., et al., *Zn–Al layered double hydroxides as chloride nanotraps in active protective coatings.* Corrosion Science, 2012. **55**(0): p. 1-4.

43. Kango, S., et al., *Surface modification of inorganic nanoparticles for development of organic–inorganic nanocomposites—A review.* Progress in Polymer Science, 2013. **38**(8): p. 1232-1261.

44. Kang, H., et al., *An effect of alginate on the stability of LDH nanosheets in aqueous solution and preparation of alginate/LDH nanocomposites.* Carbohydrate Polymers, (0).

45. *Laser Diffraction*, in *Particle Characterization: Light Scattering Methods*, B. Scarlett, Editor 2002, Springer Netherlands. p. 111-181.

46. Klug, H.P. and L.E. Alexander, *X-Ray Diffraction Procedures: For Polycrystalline and Amorphous Materials*1974: Wiley.

47. Ltd, M.I., *ZetaSizer Nano User Manual*, 2003, 2004, 2006, 2007,2008. p. 10-54.

48. International, A., *Standard Practice for Operating Salt Spray (Fog) Apparatus*2002.

49. N.LeBozec, *Accelerated corrosion tests in the automative industry: A comparison of the performance towards cosmetic corrosion.* Materials and Corrosion, 2008. **2008**: p. 889-894.

50. Echlin, P., *Handbook of Sample Preparation for Scanning Electron Microscopy and X-Ray Microanalysis*2011: Springer.

51. Macdonald, J.R., *Impedance spectroscopy.* Annals of Biomedical Engineering, 1992. **20**(3): p. 289-305.

52. V.A.Drits, A.S.B.a., *Polytype diversity of the hydrotalcite-like minerals I.Possible polytypes and theirs difraction features.* Clays and Clay Minerals, 1993. **41**: p. 551-557.

53. A.S.Bookin, V.I.C.a.V.A.D., *Polytype diversity of the hydrotalcite-like minerals II. Determination of the polytypes of experimentally studied varieties.* Clays and Clay Minerals, 1993. **41**: p. 558-564.

54. F. Kooli, I.C.C., M. Vucelic and W. Jones, *Synthesis and properties of terephthalate and benzoate intercalates of Mg-Al Layered Double Hydroxides possessing varying layer charge.* Chemistry of Materials, 1997. **8**: p. 1969 - 1977.

55. S.Miyate, *Anion-exchange properties of hydrotalcite-like compounds.* Clays and Clay Minerals, 1983. **31**(4): p. 305 - 311.

56. G.W.Brindley, C.C.K., *Structural and IR relations among brucite-like divalent metal hydroxides.* Phys. Chem. Miner, 1984. **10**: p. 187 - 191.

57. H.C.Zeng, Z.P.X.a., *Thermal evolution of Co-Hydroxides: a comparative study for their various structural phases.* Journal of Materials Chemistry, 1998. **8**: p. 2499 - 2506.

58. M.Zheludkevich, *Private Communication.*